



NATURAL RESOURCES CANADA

FALCON[®] Airborne Gravity Gradiometer Survey

Snow Lake Project, Manitoba

Project Number: 2400019

Logistics and Processing Report



Xcalibur MPH (Canada) Ltd.
6535 Millcreek Drive, Unit 35
Mississauga, Ontario, L5N 2M2
CANADA

Table of contents

1 INTRODUCTION 5

 1.1 Survey Location..... 5

 1.2 General Disclaimer..... 5

2 SUMMARY OF SURVEY PARAMETERS 6

 2.1 Survey Area Specifications 6

 2.2 Data Recording 6

 2.3 Project Safety Plan, HSE Summary 6

3 FIELD OPERATIONS 7

 3.1 Operations..... 7

 3.2 Base Stations 7

 3.2.1 GPS Base Station 7

 3.3 Personnel..... 7

4 QUALITY CONTROL RESULTS 8

 4.1 Survey Acquisition Issues 8

 4.2 Flight Path Map 8

 4.3 Turbulence 8

 4.4 AGG System Noise 9

 4.5 Digital Terrain Model 11

 4.6 Drape Surface Deviation 12

5 FALCON® AIRBORNE GRAVITY GRADIENT (AGG) RESULTS 14

 5.1 Processing Summary 14

 5.2 FALCON® Airborne Gravity Gradiometer Data..... 14

 5.3 Laser Scanner Data 14

 5.4 Positional Data 15

 5.5 Terrain Correction 15

 5.6 Tie line Levelling..... 15

 5.7 Micro-levelling 15

 5.8 Enhanced Processing 15

 5.9 FALCON® Airborne Gravity Gradient Data - G_{DD} & g_D 15

 5.9.1 Fourier Transformation 15

 5.9.2 Equivalent Source..... 16

 5.9.3 Drape Surface..... 16

 5.10 Conforming to Regional Gravity 17

 5.11 Sampling to the Database 18

6 APPENDIX I - SURVEY EQUIPMENT 19

 6.1 Survey Aircraft..... 19

 6.2 FALCON® Airborne Gravity Gradiometer 19

 6.3 Airborne Data Acquisition Systems 19

 6.4 Real-Time Differential GPS 19

 6.5 GPS Base Station Receiver 19

 6.6 Laser Scanner..... 19

6.7	Data Processing Hardware and Software	19
7	APPENDIX II - SYSTEM TESTS	20
7.1	FALCON® AGG Noise Measurement	20
7.2	Daily Calibrations and checks	20
7.2.1	FALCON® AGG Quiescent Noise Check	20
7.2.2	FALCON® AGG Calibration.....	20
8	APPENDIX III - FALCON® AGG DATA & PROCESSING	21
8.1	Nomenclature.....	21
8.2	Units	21
8.3	FALCON® Airborne Gravity Gradiometer Surveys	21
8.4	Gravity Data Processing.....	21
8.5	Aircraft Dynamic Corrections.....	22
8.6	Self-gradient Corrections.....	22
8.7	Laser Scanner Processing	22
8.8	Terrain Corrections.....	22
8.9	Tie line Levelling.....	23
8.10	Transformation into GDD & g _D	23
8.11	Terrain Corrections Using Alternate Terrain Densities	24
8.12	Noise & Signal.....	24
8.13	Risk Criteria in Interpretation	24
8.14	References.....	25
9	APPENDIX IV - DAILY REPORT.....	25
10	APPENDIX V - CALIBRATIONS.....	26
10.1	Self-gradient Calibration.....	26
10.2	Laser Scanner Calibration.....	26
11	APPENDIX VI - FINAL PRODUCTS.....	26

Figures

Figure 1: Survey Area Location 5

Figure 2: Flight Path map..... 8

Figure 3: Turbulence (milli g where $g = 9.80665 \text{ m/sec/sec}$) 9

Figure 4: System Noise NE (eotvos)..... 10

Figure 5: System Noise UV (eotvos)..... 11

Figure 6: Final Digital Terrain Model (metres, referenced to the EGM96 geoid)..... 12

Figure 7: Deviation from drape surface (metres) 13

Figure 8: FALCON® AGG Data Processing 14

Figure 9: Vertical Gravity Gradient (GDD) from Fourier processing (eotvos), terrain corrected at 2.67 g/c^3 16

Figure 10: Vertical Gravity (gD) from Fourier processing (milligal), terrain corrected at 2.67 g/c^3 17

Figure 11: Vertical Gravity (gD) from Fourier processing conformed to regional gravity data (milligal), terrain corrected at 2.67 g/c^3 18

Figure 12: **FALCON®** AGG and the gravity gradient tensor components convention 22

Tables

Table 1: Snow Lake Project – Specifications 6

Table 2: Snow Lake Project – Survey Boundary Coordinates 6

Table 3: Snow Lake Project – Personnel 7

Table 4: Snow Lake Final FALCON® AGG Digital Data – Geosoft database format 31

Table 5: Snow Lake Final FALCON® AGG Grids (Geosoft format)..... 34

1 INTRODUCTION

Xcalibur Smart Mapping conducted a high-sensitivity **FALCON**[®] Airborne Gravity Gradiometer (AGG) survey over the Snow Lake survey area under contract with Natural Resources Canada. Frank Kiss represented Natural Resources Canada during the data acquisition and data processing phases of this project.

1.1 Survey Location

The Snow Lake survey area is centred on longitude 99° 50' W, latitude 54° 44' N (see the location map in *Figure 1*). The production flights took place in March 2024 with the first production flight taking place on March 16th and the final flight taking place on March 25th. To complete the survey area coverage a total of 17 production flights were flown, with an along line resolution of 153 m. Line spacing was 400 m and tie line spacing was 2,400 m.

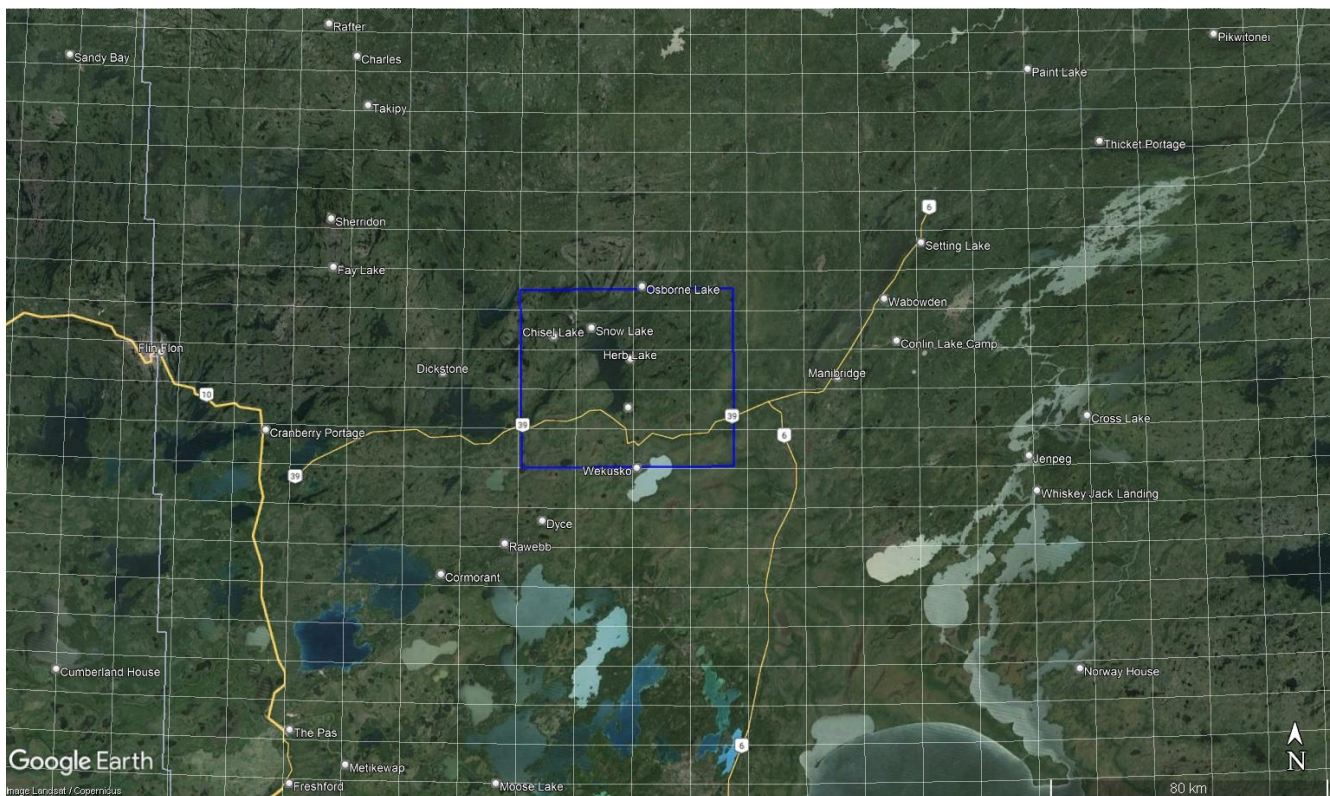


Figure 1: Survey Area Location

1.2 General Disclaimer

It is Xcalibur Smart Mapping's understanding that the data and report provided to the Client are to be used for the purpose agreed between the parties. That purpose was a significant factor in determining the scope and level of the Services being offered to the Client. Should the purpose for which the data and report are used change, the data and report may no longer be valid or appropriate and any further use of, or reliance upon, the data and report in those circumstances by the Client without Xcalibur Smart Mapping's review and advice shall be at the Client's own and sole risk.

The Services were performed by Xcalibur Smart Mapping exclusively for the purposes of the Client. Should the data and report be made available in whole or part to any third party, and such party relies thereon, that party does so wholly at its own and sole risk and Xcalibur Smart Mapping disclaims any liability to such party.

Where the Services have involved Xcalibur Smart Mapping's use of any information provided by the Client or third parties, upon which Xcalibur Smart Mapping was reasonably entitled to rely, then the Services are limited by the accuracy of such information. Xcalibur Smart Mapping is not liable for any inaccuracies (including any incompleteness) in the said information, save as otherwise provided in the terms of the contract between the Client and Xcalibur Smart Mapping.

2 SUMMARY OF SURVEY PARAMETERS

2.1 Survey Area Specifications

Total Kilometres all lines (km)	8,920.8
Clearance Method	Drape
Minimum Drape Height (m)	80
Traverse Line Direction (deg.)	90 / 270
Traverse Line Spacing (m)	400
Tie Line Direction (deg.)	0 / 180
Tie Line Spacing (m)	2,400

Table 1: Snow Lake Project – Specifications

The survey block is defined by the coordinates in *Table 2*, in geographical coordinates, referenced to the NAD83 datum.

Id	LONG	LAT
1	-100.14.18	54.29.58
2	-100.15.08	54.57.08
3	-99.18.33	54.57.30
4	-99.18.21	54.30.19

Table 2: Snow Lake Project – Survey Boundary Coordinates

2.2 Data Recording

The following parameters were recorded during the course of the survey:

- **FALCON® AGG data:** recorded at different intervals.
- **Terrain clearance:** provided by the radar altimeter at intervals of 0.1 s.
- **Airborne GPS positional data** (latitude, longitude, height, time and raw range from each satellite being tracked): recorded at intervals of 1 s.
- **Time markers:** in digital data.
- **Ground based GPS positional data** (latitude, longitude, height, time and raw range from each satellite being tracked): recorded at intervals of 1 s.
- **Ground surface below aircraft:** mapped by the laser scanner system (when within range of the instrument and in the absence of thick vegetation), scanning at 36 times per second, recording 276 returns per scan.

2.3 Project Safety Plan, HSE Summary

A Job Safety Plan and Job Safety Analysis was prepared and implemented in accordance with the [Xcalibur Smart Mapping](#) Occupational Safety and Health Management System.

3 FIELD OPERATIONS

3.1 Operations

The survey was based out of Flin Flon, Manitoba, Canada. The survey aircraft was operated from Flin Flon Airport using aviation fuel available on site. A temporary office was set up in Victoria Inn where all survey operations were run, and the post-flight data verification was performed.

3.2 Base Stations

A dual frequency GPS base station was set up in order to correct the raw GPS data collected in the aircraft. A secondary GPS base station was available but was not required.

3.2.1 GPS Base Station

Location: Flin Flon Airport
 Date: March 16th, 2024
 Latitude: 54° 40' 38.28505" N
 Longitude: 101° 40' 43.42894" W
 Height: 269.970 m ellipsoidal

3.3 Personnel

The following technical personnel participated in survey operations:

Crew Leader:	A. Malik
Pilots:	S. Parks, R. Linto, J. Clayton
AME:	A. Ott
Technicians:	A. Malik
Project Manager:	B. Robinson
QC and Processing:	K. Chase, P. Cassidy

Table 3: Snow Lake Project – Personnel

4 QUALITY CONTROL RESULTS

4.1 Survey Acquisition Issues

During the course of the survey, there were no data quality issues with:

- AGG instrumentation
- GPS base stations
- Data acquisition systems
- Laser scanner

4.2 Flight Path Map

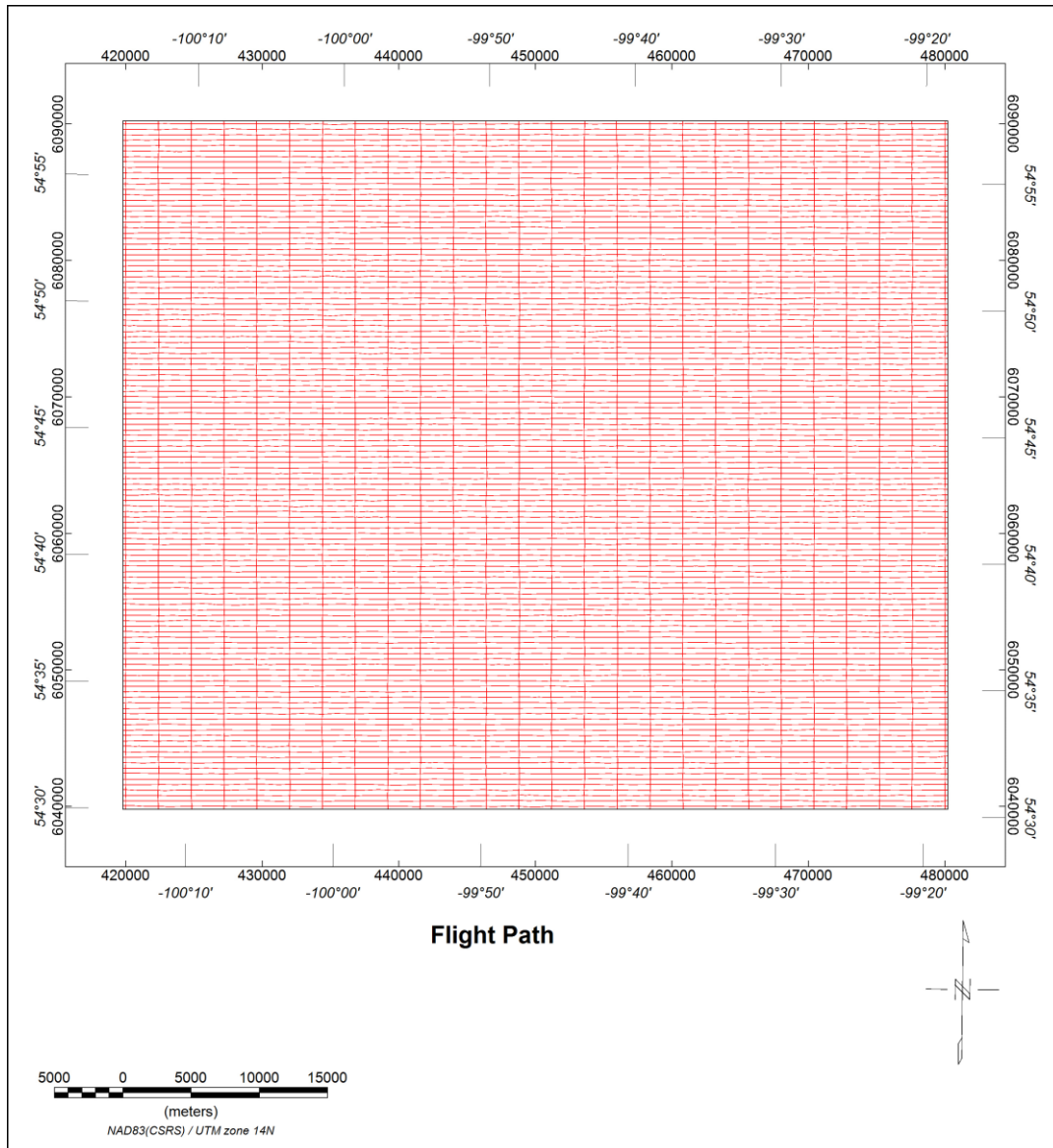


Figure 2: Flight Path map

4.3 Turbulence

The mean turbulence recorded in the Snow Lake survey area was 72 milli g (where $g = 9.80665 \text{ m/sec/sec}$). Turbulence was variable, ranging from very low to high. The typical pattern for a given day was for turbulence to increase and decrease with daily temperature. The turbulence pattern across the survey area is shown in *Figure 3*.

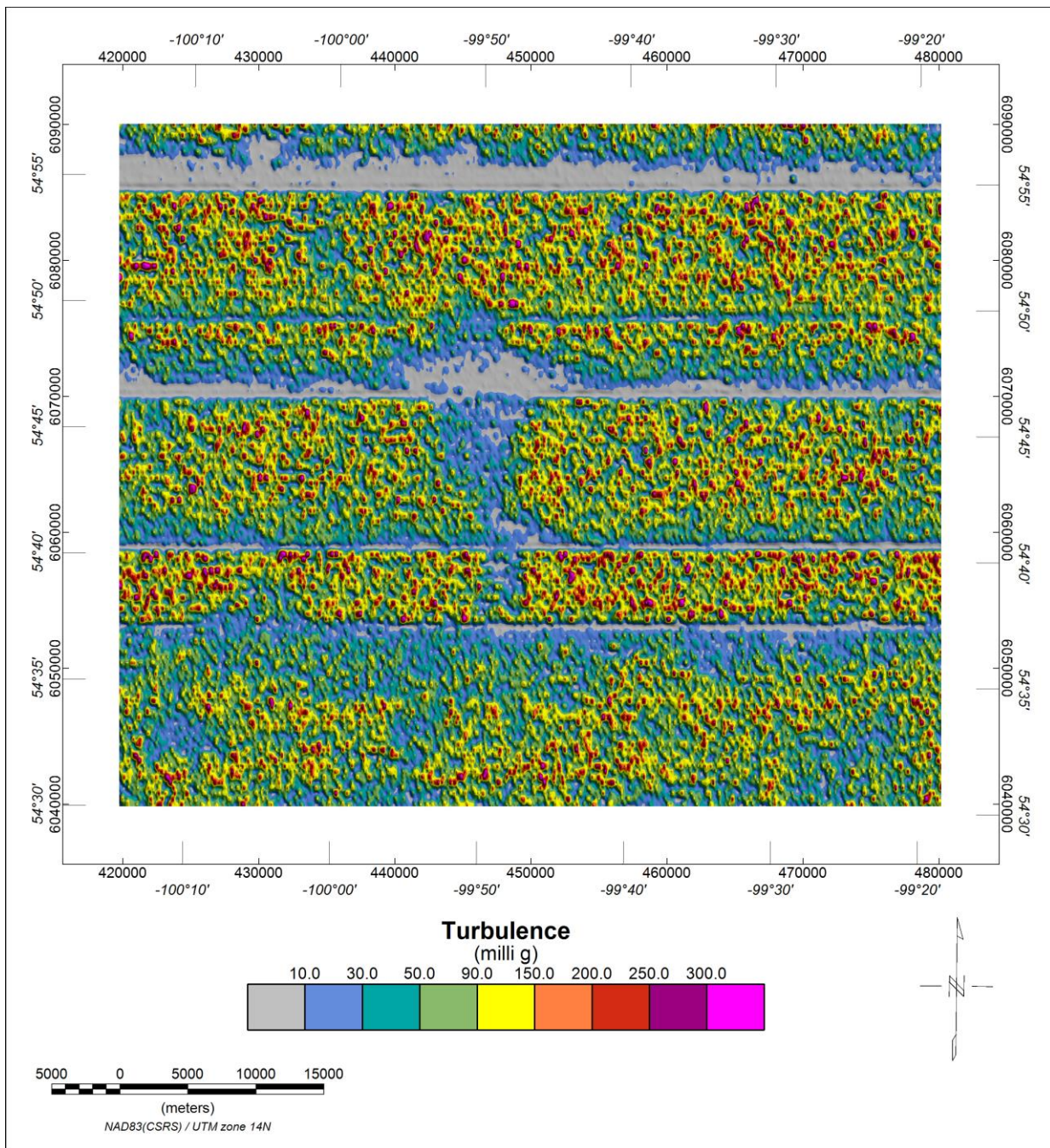


Figure 3: Turbulence (milli g where $g = 9.80665 \text{ m/sec/sec}$)

4.4 AGG System Noise

The system noise is defined to be the standard deviation of half the difference between the A & B complements, for each of the NE and UV curvature components. The results for this survey had values of 3.0 E and 3.0 E for NE and UV respectively.

Figure 4 and Figure 5 provide a representation of the variation in this standard deviation for each component. This is achieved by gridding a rolling measurement of standard deviation along each line using a window length of 100 data points.

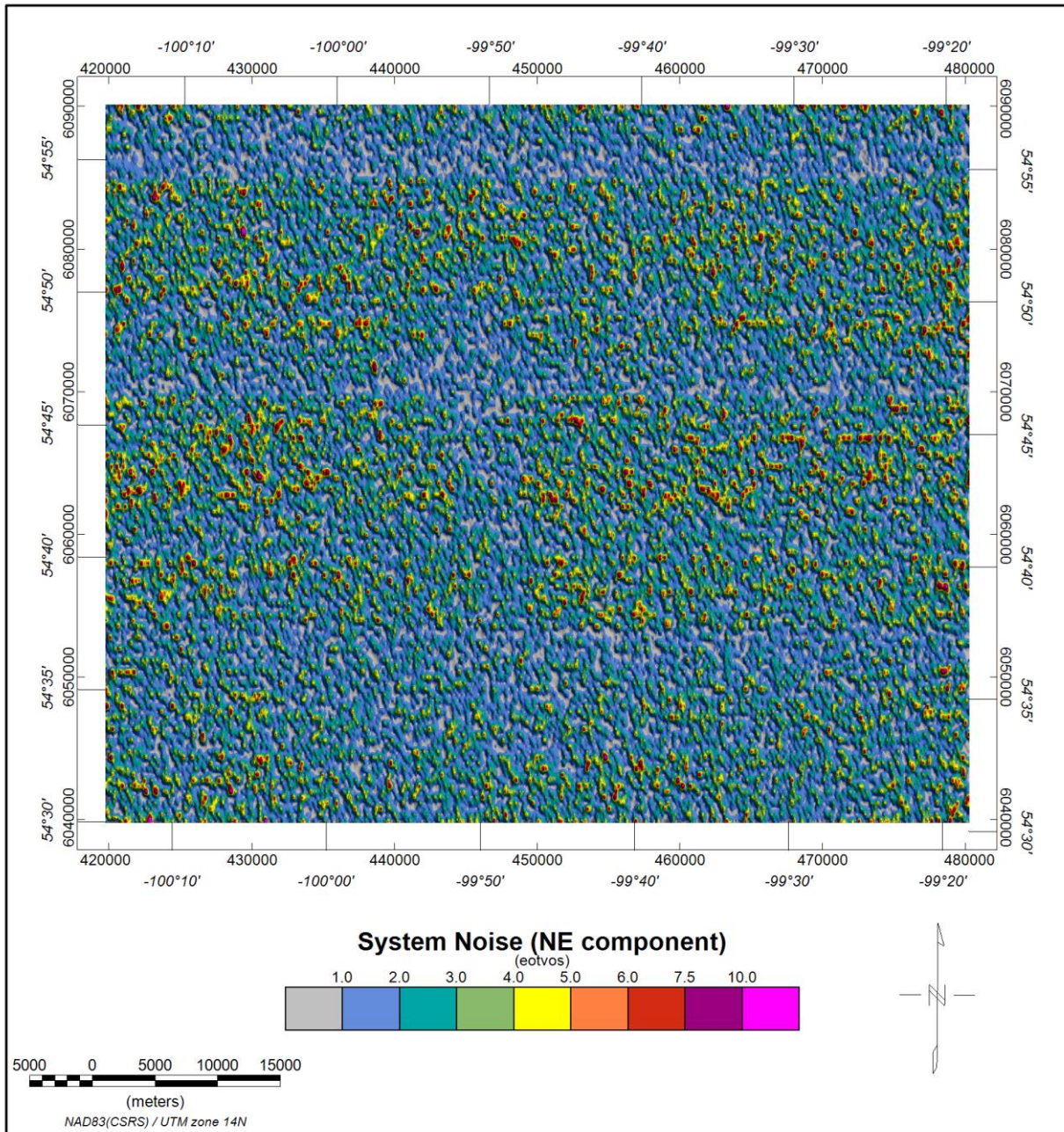


Figure 4: System Noise NE (eotvos)

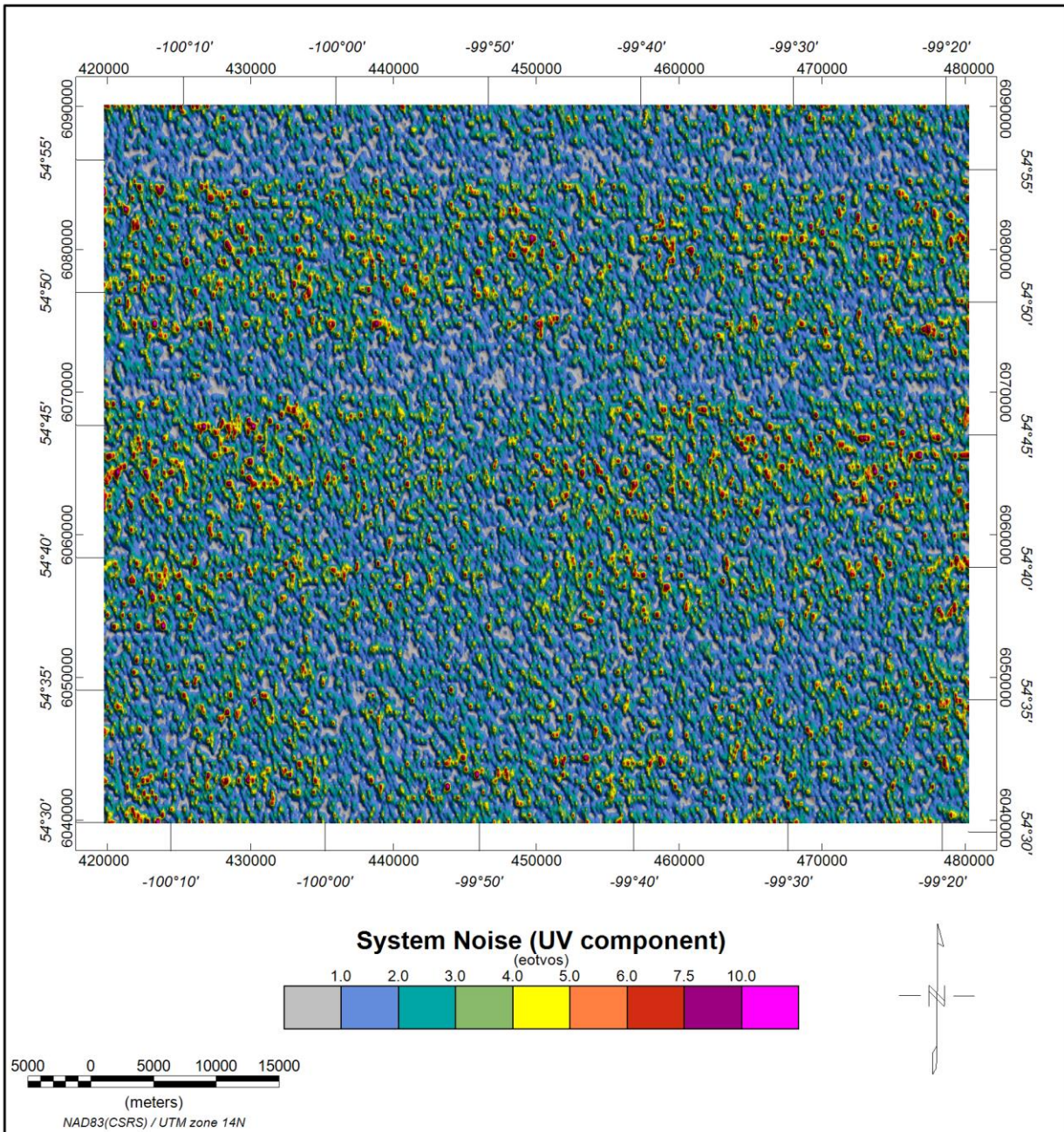


Figure 5: System Noise UV (eotvos)

4.5 Digital Terrain Model

Laser scanner data quality was good with scan density generally above 90%. Laser scanner data were gridded at 15 m with a 1 cell maximum extension beyond data limits. To fill gaps between lines and extend data coverage beyond the survey area, TanDEM-X (TerraSAR-X add-on for Digital Elevation Measurement) (one arc second resolution) grid data were excised to an area 65 km beyond the planned survey area. The excised data were adjusted to the level of the laser scanner data using a grid difference adjustment method. The two grids were then combined into a single grid such that unmodified laser scanner data were used where defined and adjusted TanDEM-X data were used to fill the gaps and extend the area. *Figure 6* shows the final Digital Terrain Model (referenced to the EGM96 geoid) for the survey area.

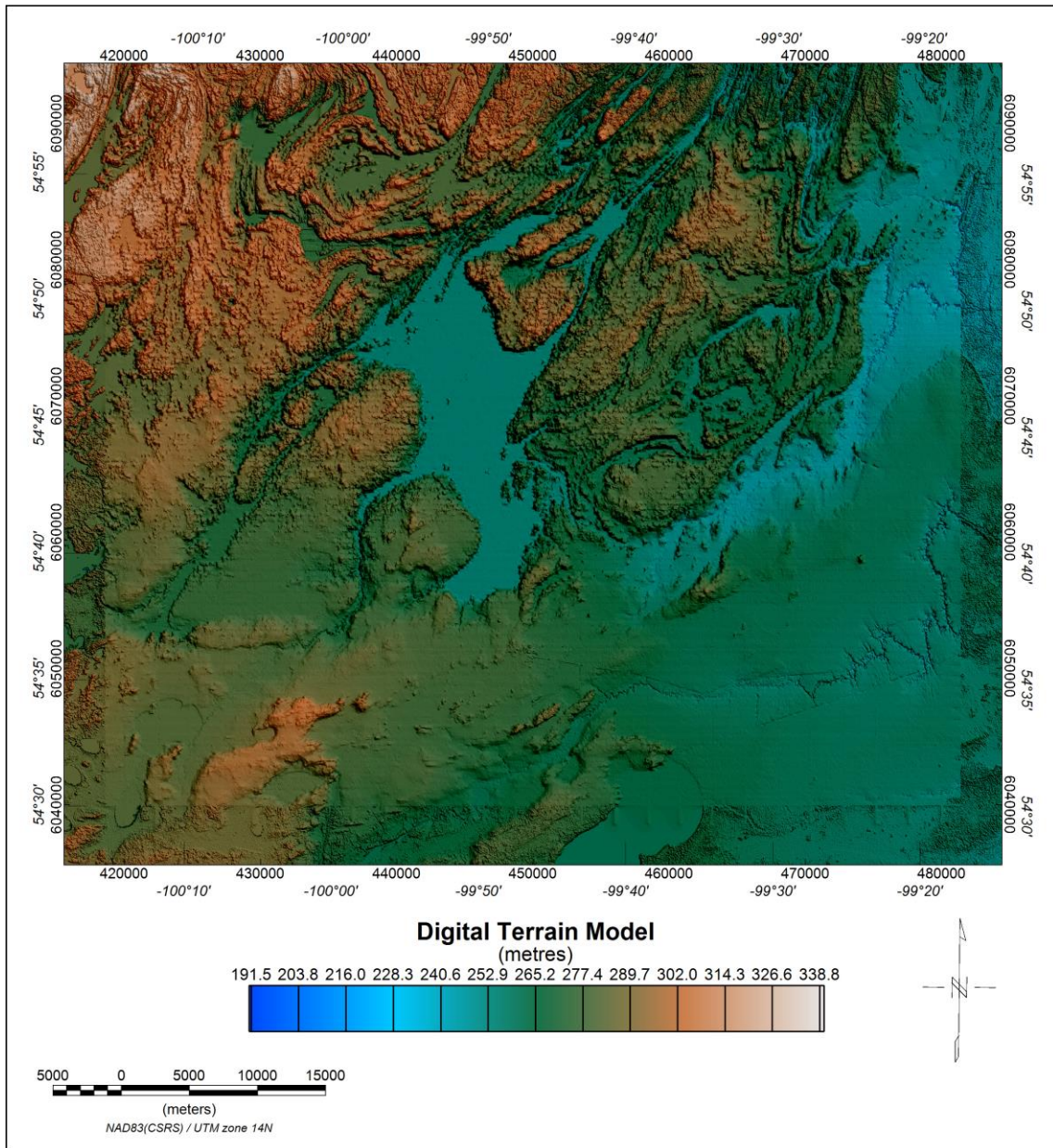


Figure 6: Final Digital Terrain Model (metres, referenced to the EGM96 geoid)

4.6 Drape Surface Deviation

Flying height for the Snow Lake survey was determined by a pre-computed “drape surface”; designed to create a smooth flight surface, maximising both acquisition quality and safety. The average deviation of actual flying height from this surface was 0.9 m across the survey area. The deviation is shown in *Figure 7*.

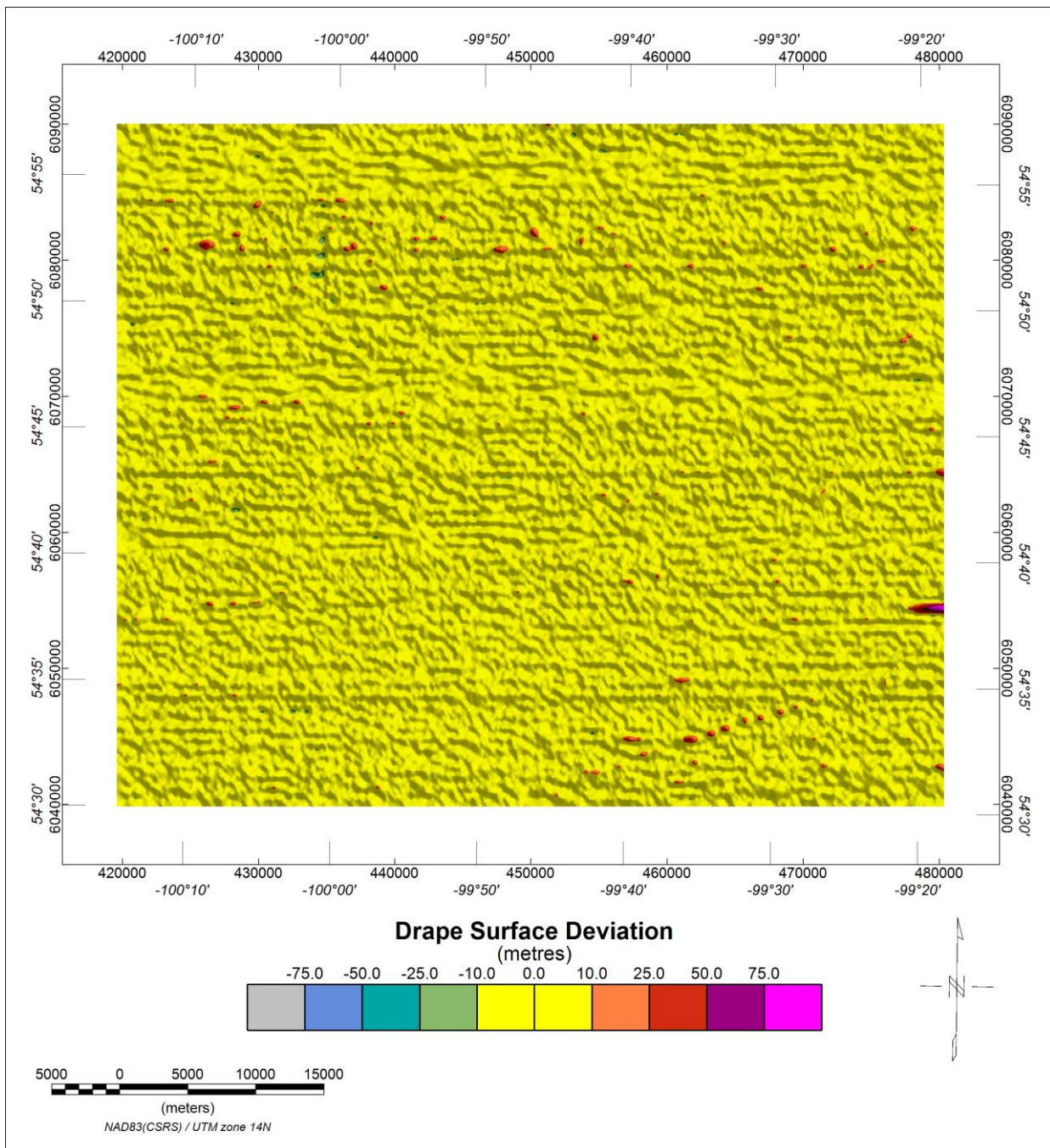


Figure 7: Deviation from drape surface (metres)

5 FALCON[®] AIRBORNE GRAVITY GRADIENT (AGG) RESULTS

5.1 Processing Summary

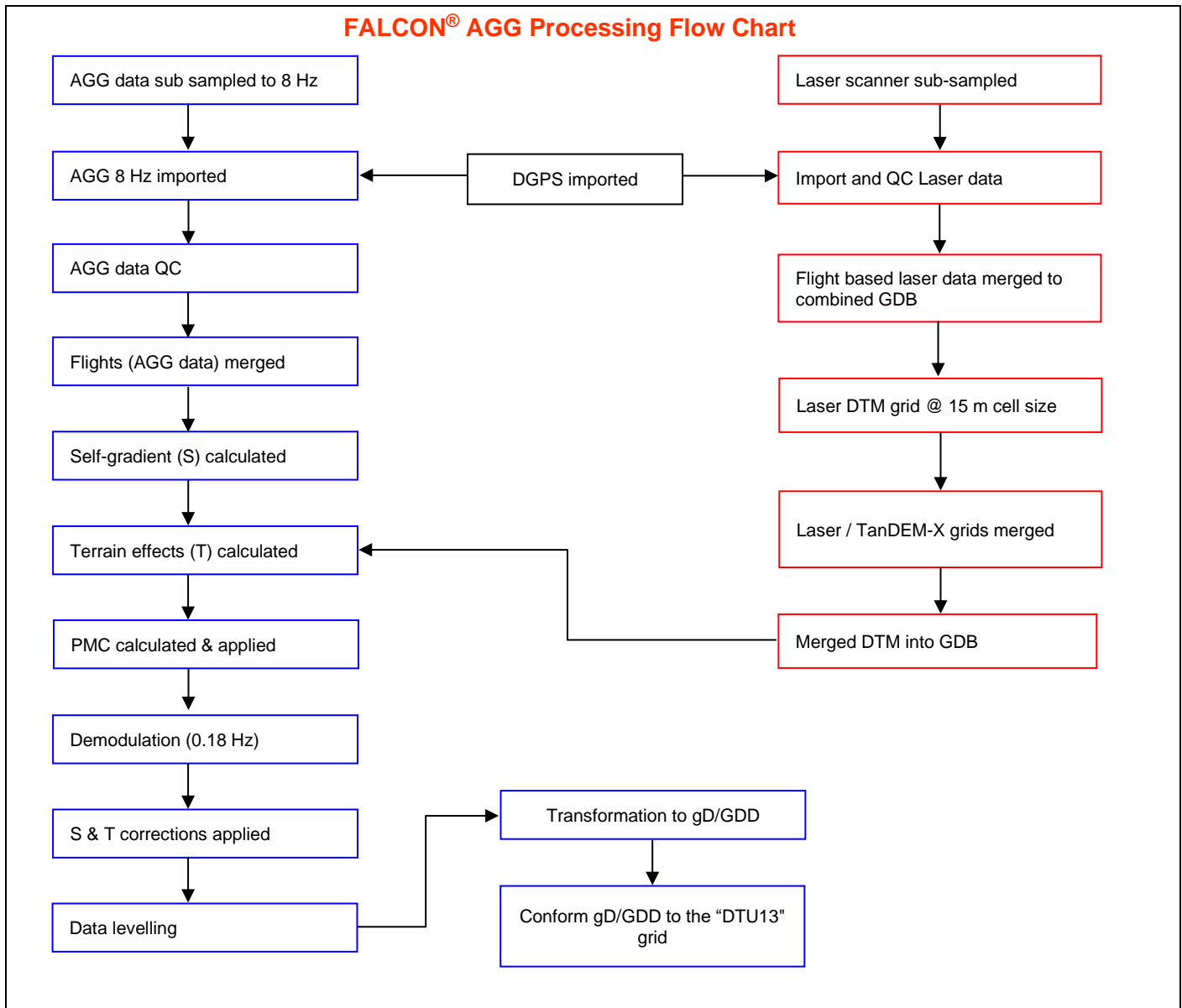


Figure 8: FALCON[®] AGG Data Processing

5.2 FALCON[®] Airborne Gravity Gradiometer Data

Figure 8 summarises the steps involved in processing the AGG data obtained from the survey.

The FALCON[®] Airborne Gravity Gradiometer data were digitally recorded by the ADAS on removable hard drives. The raw data were then copied to the field processing laptop, backed up twice onto hard disk media and transferred by Secure File Transfer to the Xcalibur Smart Mapping's secure server.

Preliminary processing and QC of the FALCON[®] AGG data were completed on-site using Xcalibur Smart Mapping's AGG QC software. Further QC and final FALCON[®] AGG data processing were performed by the office-based data processor.

5.3 Laser Scanner Data

Laser scanner returns were recorded at a rate of 36 scans per second with each scan returning 276 data points. Each return was converted to ground surface elevation by combining scanner range and angle data with aircraft position and attitude data. Computed elevations were then sub sampled by first dividing each scan into ten segments and combining five adjacent

scans per segment, then using a special algorithm to select the optimum return within each data "bin" thus formed. Sub-sampled laser scanner data were edited to remove spikes prior to gridding.

5.4 Positional Data

Differential GPS processing was applied to compute accurate aircraft positions once per second. Waypoint's GrafNav GPS processing software calculated DGPS positions using raw range data obtained from receivers in the aircraft and at a fixed ground base station.

The GPS ground station position was determined by sending several hours of collected data to an online GPS processing service to obtain a differentially corrected computed position. The service selected was CSRS-PPP, which is provided by Natural Resources Canada. The GPS data were processed and quality controlled using the WGS84 datum.

Parameters for the WGS84 datum are:

Ellipsoid: WGS84

Semi-major axis: 6,378,137.0 m

Inverse flattening (1/f): 298.257

All processing was performed using WGS84/UTM Zone 14N coordinates. Final line data and final grid data were supplied in NAD83/UTM Zone 14N.

5.5 Terrain Correction

Terrain corrections were derived from the digital terrain model grid for every data point in the survey. A terrain density of 1.00 g/cm³ was used to compute the terrain correction channels, which were then multiplied by the chosen correction density before being subtracted from the data.

In consultation with the Client, a correction density of 2.95 g/cm³ was selected as approximating most closely the density of the terrain in the survey area and was applied. As standard, a density of 2.67 g/cm³ was also applied and these data are also included. An alternative method for computing terrain corrected data for additional densities is described in section 8.11.

5.6 Tie line Levelling

The terrain corrected data and the uncorrected data were then tie line levelled.

5.7 Micro-levelling

Micro-levelling was applied to the levelled data to remove residual levelling errors.

5.8 Enhanced Processing

The enhanced processing technique improves the noise amplitude density (as discussed by Christensen et al, 2015) by 25-50% for surveys with line spacing of less than 1 km. The method exploits the different spatial frequencies of system noise and geologic signal. After converting the data into the 2D spatial domain, a custom spatial filter is applied that removes the system noise, while retaining the remaining geologic signal. The process will limit the data resolution to the survey line spacing. The Falcon Difference Noise of the standard product is 3.0 E at 153 m resolution and after applying the processing enhancement, the Falcon Difference Noise is reduced to 2.1 E at 400 m resolution. Calculating the noise amplitude density is a more appropriate means to evaluate noise with data at different resolutions, which is calculated from the [A,B][NE,UV] channels. The standard product has a noise amplitude density of 1.66 E $\sqrt{\text{km}}$ and the enhanced product has a noise amplitude density of 1.48 E $\sqrt{\text{km}}$.

5.9 FALCON[®] Airborne Gravity Gradient Data - G_{DD} & g_D

The transformation into G_{DD} and g_D was accomplished using a Fourier domain transformation method and an equivalent source method.

5.9.1 Fourier Transformation

The Fourier domain transformation method firstly calculates many flat surfaces at constant intervals between the lowest and highest-flying altitude. The transformation is performed on each of these surfaces and the result is a three-dimensional array for each tensor component where each level corresponds to a flat layer of a constant flying height. Using an approximation, the data is interpolated from this array back onto the processing drape surface.

5.9.2 Equivalent Source

The equivalent source transformation utilises a smooth model inversion to calculate the density of a surface of sources followed by a forward calculation to produce g_D and the gravity gradient tensor components. The sources were placed at a depth of 300 metres.

5.9.3 Drape Surface

The Fourier transformation uses a smoothed surface (DRAPE_FFT) onto which the output data are projected. This Fourier surface is a smoother equivalent of the actual flying surface (GPSALT), which is smoothed using a filter based on flying height and line spacing. The equivalent source drape is equal to the Fourier drape (DRAPE_FFT=DRAPE_EQS).

The Fourier G_{DD} (terrain corrected at 2.67 g/c^3) map is shown in *Figure 9*.

The Fourier vertical gravity (g_D), derived by integrating G_{DD} , (terrain corrected at 2.67 g/c^3) result is presented in *Figure 10*.

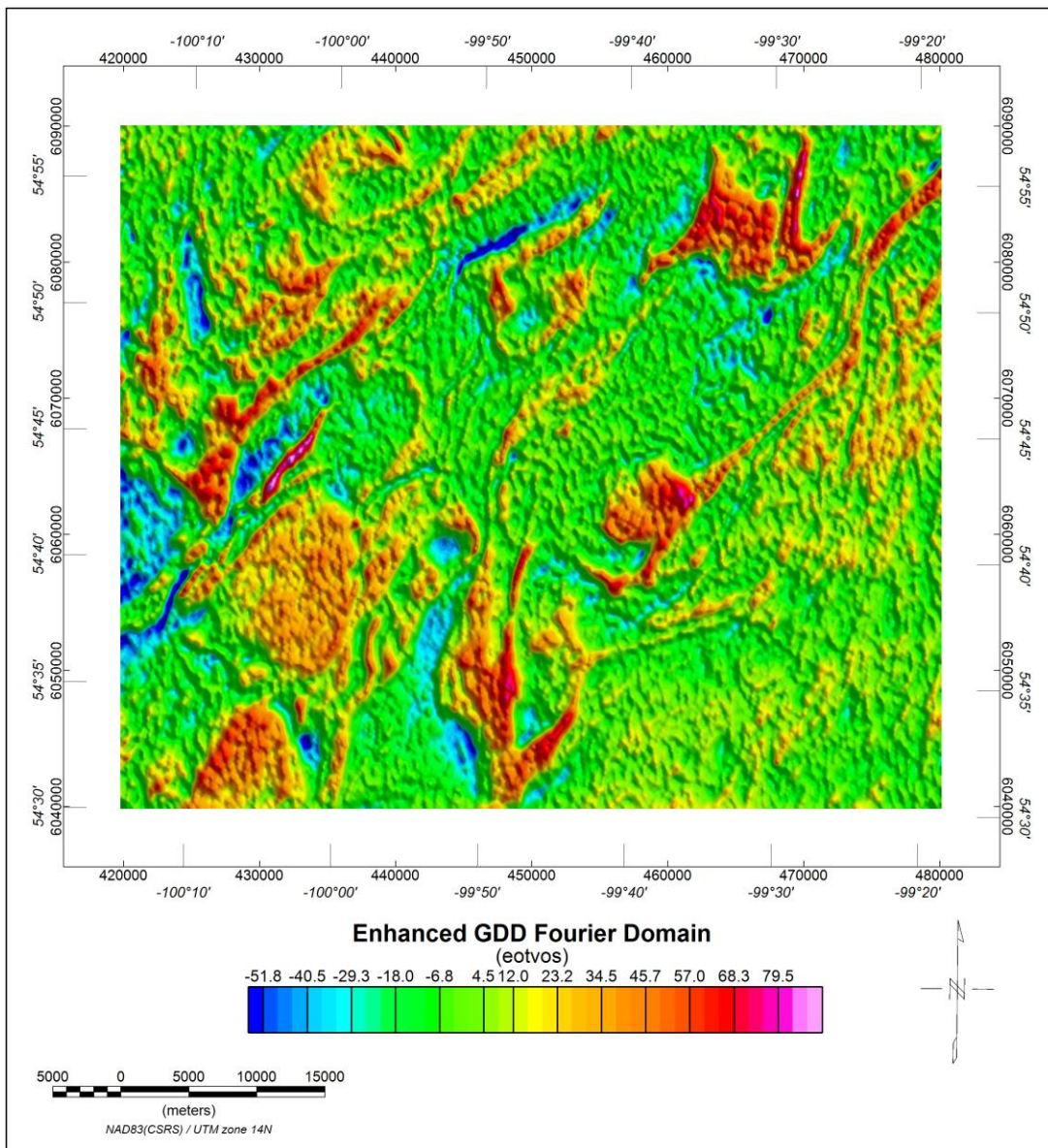


Figure 9: Vertical Gravity Gradient (GDD) from Fourier processing (eotvos), terrain corrected at 2.67 g/c^3

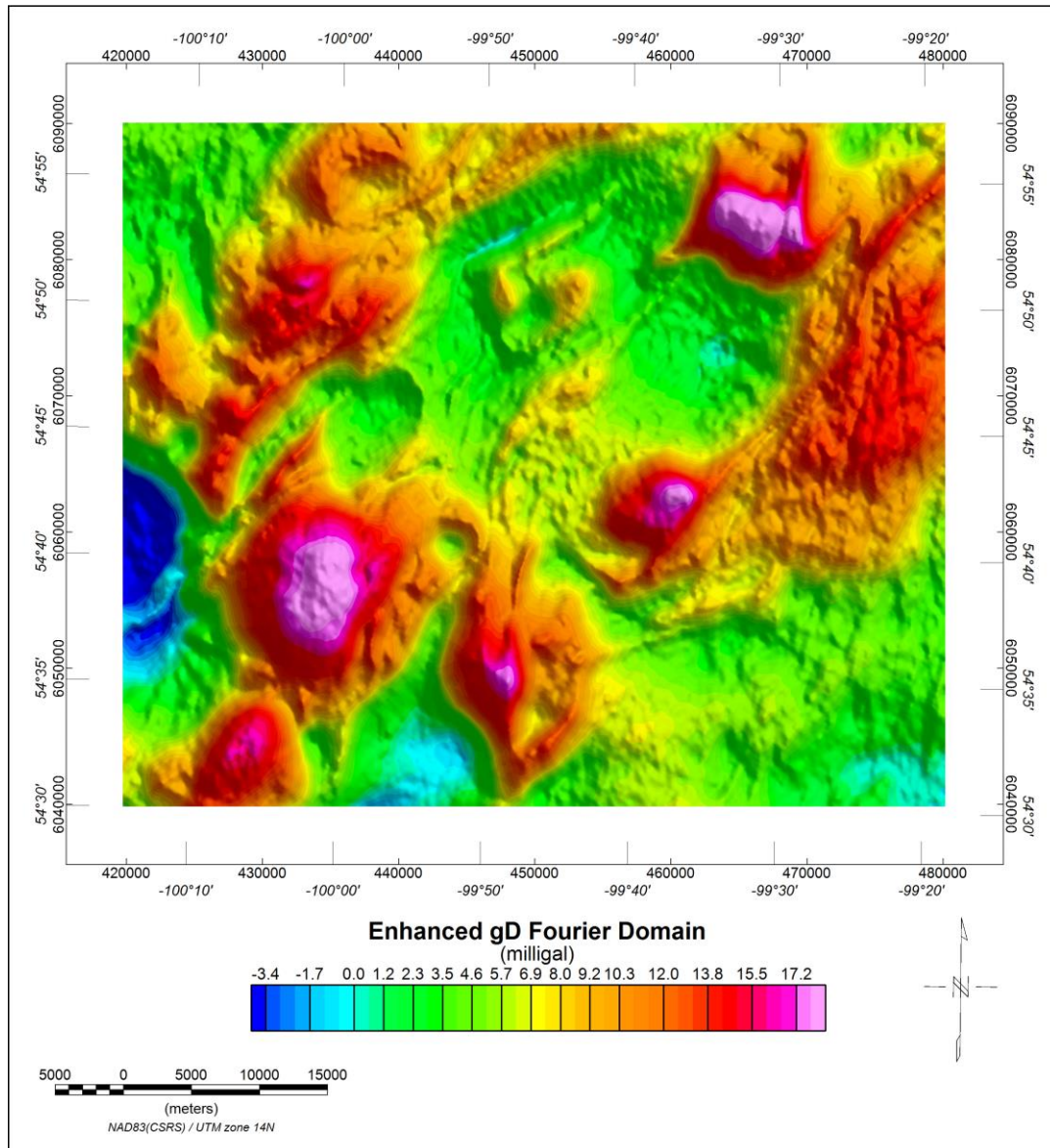


Figure 10: Vertical Gravity (gD) from Fourier processing (milligal), terrain corrected at 2.67 g/c^3

5.10 Conforming to Regional Gravity

As discussed in section 8.3, the long wavelength information in g_D and G_{DD} can be improved by incorporating ancillary information. Such information is available in the form of the Danish Technical University global gravity data of 2013 (DTU13) grids.

The g_D and G_{DD} grids were conformed to grids derived from a subset of the DTU13 grids as follows. The g_D (terrain corrected at 2.67 g/c^3) results are presented in *Figure 11*.

- Low pass filter the regional data using a cosine squared filter with cut-off at 30 km, tapering to 20 km.
- High pass filter the g_D and G_{DD} data using a cosine squared filter with cut-off at 30 km, tapering to 20 km.
- Conform the g_D and G_{DD} data to the regional data by addition of the filtered grids. The filter design is such that this method provides uniform frequency response across the overlap frequencies.

Further discussion of this method can be found in Dransfield (2010).

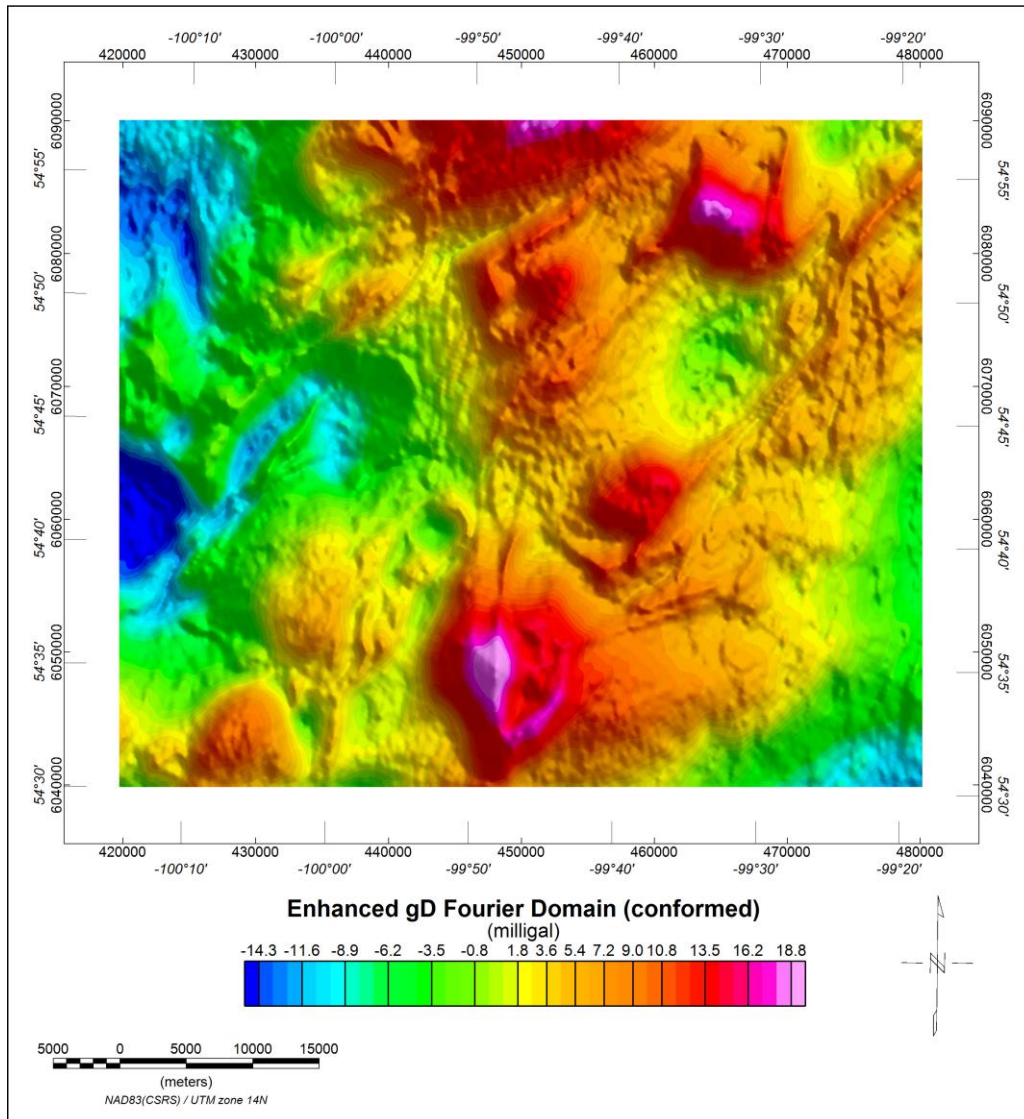


Figure 11: Vertical Gravity (gD) from Fourier processing conformed to regional gravity data (milligal), terrain corrected at 2.67 g/c³

5.11 Sampling to the Database

The unconformed and conformed grids were then sampled into the database to provide the gravity and gravity gradient channels. The tie line data were not used in the gridding process to make the delivered grids. To populate the tie line gravity and gravity gradient channels in the database, a set of unconformed grids were made, which did include all lines in the gridding process, and these grids were sampled to populate the unconformed and conformed tie line channels in the database.

6 APPENDIX I - SURVEY EQUIPMENT

6.1 Survey Aircraft

An **Xcalibur Smart Mapping** Cessna C208B turbo prop, Canadian registration C-GGRD was used to fly the survey area. The following instrumentation was used for this survey.

6.2 FALCON[®] Airborne Gravity Gradiometer

FALCON[®] AGG Analog System (Galileo)

The **FALCON[®] AGG** System is based on current state-of-the-art airborne gravity gradiometer technology and has been optimized for airborne broadband geophysical exploration. The system is capable of supporting surveying activities in areas ranging from 1,000 ft below sea level to 13,000 ft above sea level with aircraft speeds from 30 to 130 knots. The **FALCON[®] AGG** data streams were recorded at different rates on removable drives installed in the **FALCON[®] AGG** electronics rack.

6.3 Airborne Data Acquisition Systems

FALCON[®] AGG Data Acquisition System (ADAS)

The **ADAS** provides control and data display for the **FALCON[®] AGG** system. Data are displayed in real time for the operator and warnings displayed should system parameters deviate from tolerance specifications. All **FALCON[®] AGG** and laser scanner data are recorded to a removable hard drive.

6.4 Real-Time Differential GPS

The **Novatel OEMV-3G** multi-frequency positioning receiver provides real-time differential GNSS for the on-board navigation system. The **OEMV-3** is designed to track the GPS L1 and L2 signals, as well as GLONASS L1 and L2. The differential data set is relayed via a geo-synchronous satellite to the aircraft where the receiver optimized the corrections for the current location.

6.5 GPS Base Station Receiver

The **Javad Triumph-M1** is a 216-channel, multi-frequency GNSS receiver. It can provide raw range information of all satellites in view from the GPS, GLONASS, BeiDou and Galileo satellite systems. The receiver can sample at up to 5 Hz and records to internal memory. These data are used to provide post-processed differential GNSS (DGNSS) corrections for the rover data flight path.

6.6 Laser Scanner

Riegl LMS-Q240I-60

The laser scanner is designed for high-speed line scanning applications. The system is based upon the principle of time-of-flight measurement of short laser pulses in the infrared wavelength region and the angular deflection of the laser beam is obtained by a rotating polygon mirror wheel. The measurement range is up to 650 m with a minimum range of 2 m and an accuracy of 20 mm. The laser beam is eye safe; the laser wavelength is 0.9 μm , the scan angle range is +/- 40° and the scan speed is 36 scans/s.

6.7 Data Processing Hardware and Software

The following equipment and software were used:

Hardware

- One 2.0 GHz (or higher) laptop computer
- External USB hard drive reader for ADAS removable drives
- Two External USB hard drives for data backup

Software

- Oasis Montaj data processing and imaging software
- GrafNav Differential GPS processing software
- **Xcalibur Smart Mapping's** Atlas data processing software
- **Xcalibur Smart Mapping's** DiAGG processing software

7 APPENDIX II - SYSTEM TESTS

7.1 FALCON® AGG Noise Measurement

At the commencement of the survey, 20 minutes of data were collected with the aircraft in straight level flight at 3500 ft AGL. These data were assessed in-flight to check the AGG noise levels.

Daily flight debriefs incorporating **FALCON®** AGG performance statistics for each flight line are prepared using output from Xcalibur Smart Mapping's DiAGG software. These are sent daily to Xcalibur Smart Mapping's office staff for performance evaluation.

7.2 Daily Calibrations and checks

A set of daily calibrations and checks were performed each survey day as follows:

7.2.1 FALCON® AGG Quiescent Noise Check

Prior to each day's survey, the AGG quiescent noise levels were checked to verify the system was performing as expected.

7.2.2 FALCON® AGG Calibration

A calibration was performed at the beginning of each flight and the results monitored by the operator. The coefficients obtained from each of the calibrations were used in the processing of the data.

8 APPENDIX III - FALCON[®] AGG DATA & PROCESSING

8.1 Nomenclature

The FALCON[®] airborne gravity gradiometer (AGG) system adopts a North, East, and Down coordinate sign convention and these directions (N, E, and D) are used as subscripts to identify the gravity gradient tensor components (gravity vector derivatives). Lower case is used to identify the components of the gravity field and upper case to identify the gravity gradient tensor components. Thus, the parameter usually measured in a normal exploration ground gravity survey is g_D and the vertical gradient of this component is G_{DD} .

8.2 Units

The vertical component of gravity (g_D) is delivered in the usual units of mGal. The gradient tensor components are delivered in eotvos, which is usually abbreviated to “E”. By definition $1 \text{ E} = 10^{-4} \text{ mGal/m}$.

8.3 FALCON[®] Airborne Gravity Gradiometer Surveys

In standard ground gravity surveys, the component measured is “ g_D ”, which is the *vertical component of the acceleration due to gravity*. In airborne gravity systems, since the aircraft is itself accelerating, measurement of “ g_D ” cannot be made to the same precision and accuracy as on the ground. Airborne gravity gradiometry uses a differential measurement to remove the aircraft motion effects and delivers gravity data of a spatial resolution and sensitivity comparable with ground gravity data.

The FALCON[®] gradiometer instrument acquires two curvature components of the gravity gradient tensor namely G_{NE} and G_{UV} where $G_{UV} = (G_{NN} - G_{EE})/2$.

A feature of the FALCON[®] AGG system is that two independent measurements are made of both the NE and UV curvature components. This is achieved by using two sets of accelerometers, referred to as the A complement and the B complement. Each complement consists of four accelerometers. The measured gradients from these complements are referred to as A_{NE} and A_{UV} and B_{NE} and B_{UV} . The G_{NE} and G_{UV} gradients are computed by averaging A and B:

$$G_{NE} = \frac{(A_{NE} + B_{NE})}{2}$$

$$G_{UV} = \frac{(A_{UV} + B_{UV})}{2}$$

Since these curvature components cannot easily and intuitively be related to the causative geology, they are transformed into the vertical gravity gradient (G_{DD}) and integrated to derive the vertical component of gravity (g_D). Interpreters display, interpret, and model both G_{DD} and g_D . The directly measured G_{NE} and G_{UV} data are appropriate for use in inversion software to generate density models of the earth. The vertical gravity gradient, G_{DD} , is more sensitive to small or shallow sources and has greater spatial resolution than g_D (similar to the way that the vertical magnetic gradient provides greater spatial resolution and increased sensitivity to shallow sources of the magnetic field). In the integration of G_{DD} to give g_D , the very long wavelength component, at wavelengths comparable to or greater than the size of the survey area, cannot be fully recovered. Long wavelength gravity data are therefore incorporated in the g_D data from other sources. This might be regional ground, airborne or marine gravity if such data are available. The Danish Technical University global gravity data of 2013 (DTU13) are used as a default if other data are not available.

8.4 Gravity Data Processing

The main elements and sequence of processing of the gravity data are given below. Unless not applicable or specified otherwise, the processing step is applied to each individual complement element (A_{NE} , A_{UV} , B_{NE} , B_{UV}):

1. Dynamic corrections for residual aircraft motion (called Post Mission Compensation or PMC) are calculated and applied.
2. Self-gradient corrections are calculated and applied to reduce the time-varying gradient response from the aircraft and platform.
3. A Digital Terrain Model (DTM) is created from the laser scanner range data, the AGG inertial navigation system rotation data and the DGPS position data.
4. Terrain corrections are calculated and applied.
5. Line levelling and micro-levelling (where necessary) are applied.
6. G_{NE} and G_{UV} are transformed into the full gravity gradient tensor, including G_{DD} , and into g_D .

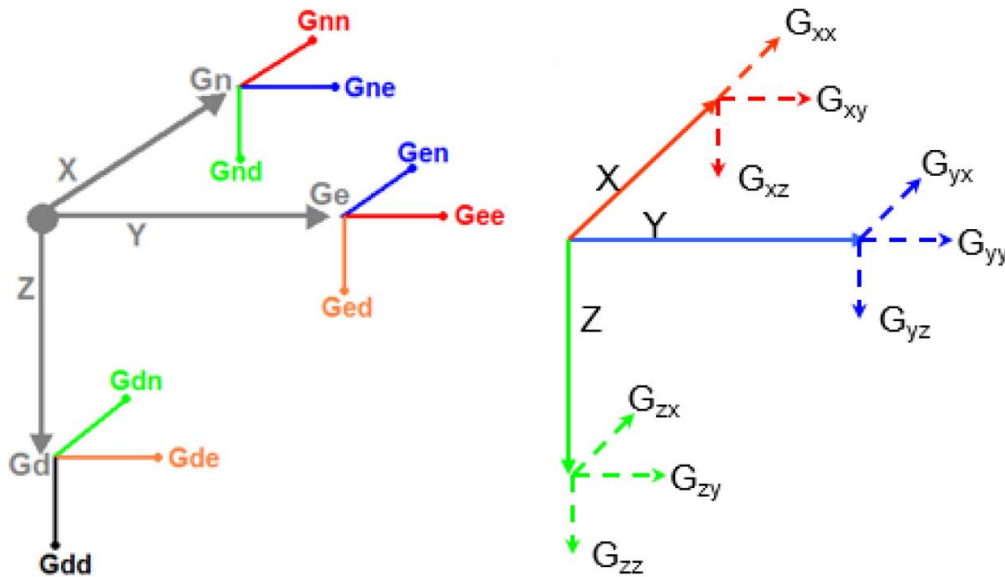


Figure 12: FALCON[®] AGG and the gravity gradient tensor components convention

8.5 Aircraft Dynamic Corrections

The design and operation of the FALCON[®] AGG results in very considerable reduction of the effects of aircraft acceleration, but residual levels are still significant and further reduction is required and must be done in post-processing.

Post-processing correction relies on monitoring the inertial acceleration environment of the gravity gradiometer instrument (GGI) and constructing a model of the response of the GGI to this environment. Parameters of the model are adjusted by regression to match the sensitivity of the GGI during data acquisition. The modelled GGI output in response to the inertial sensitivities is subtracted from the observed output. Application of this technique to the output of the GGI, when it is adequately compensated by its internal mechanisms, reduces the effect of aircraft motion to acceptable levels.

Following these corrections, the gradient data are demodulated and filtered along line using a 6-pole Butterworth low-pass filter with a cut-off frequency of 0.18 Hz.

8.6 Self-gradient Corrections

The GGI is mounted in gimbals controlled by an inertial navigation system, which keeps the GGI pointing in a fixed direction whilst the aircraft and gimbals rotate around it. Consequently, the GGI measures a time-varying gravity gradient due to these masses moving around it as the heading and attitude of the aircraft changes during flight. This is called the self-gradient.

Like the aircraft dynamic corrections, the self-gradient is calculated by regression of model parameters against measured data. In this case, the rotations of the gimbals are the input variables of the model. Once calculated, the modelled output is subtracted from the observed output.

8.7 Laser Scanner Processing

The laser scanner measures the range from the aircraft to the ground in a swath of angular width ± 80 degrees below the aircraft. The aircraft attitude (roll, pitch and heading) data provided by the AGG inertial navigation system are used to adjust the range data for changes in attitude and the processed differential GPS data are used to reference the range data to located ground elevations referenced to the WGS84 datum (corrected for the EGM96 geoid separation model). Statistical filtering strategies are used to remove anomalous elevations due to foliage or built-up environment. The resulting elevations are gridded to form a digital terrain model (DTM).

8.8 Terrain Corrections

An observation point above a hill has excess mass beneath it compared to an observation point above a valley. Since gravity is directly proportional to the product of the masses, uncorrected gravity data have a high correlation with topography.

It is therefore necessary to apply a terrain correction to gravity survey data. For airborne gravity gradiometry at low survey heights, a detailed DTM is required. Typically, immediately below the aircraft, the digital terrain will need to be sampled at a cell size roughly one-third to one-half of the survey height and with a position accuracy of better than 1 metre. For these accuracies, LIDAR data are required and each **FALCON**[®] survey aircraft comes equipped with LIDAR (laser scanner).

If bathymetric data are used, then these form a separate terrain model for which terrain corrections are calculated at a density chosen to suit the water bottom – water interface.

Once the DTM has been merged, the terrain corrections for each of the **G_{NE}** and **G_{UV}** data streams are calculated. In the calculation of terrain corrections, a density of 1 g/cm³ is used. The calculated corrections are stored in the database allowing the use of any desired terrain correction density by subtracting the product of desired density and correction from the measured **G_{NE}** and **G_{UV}** data. The terrain correction density is chosen to be representative of the terrain density over the survey area. Sometimes more than one density is used with input from the Client.

Typically, the terrain corrections are calculated over a distance 40 to 60 km from each survey measurement point.

8.9 Tie line Levelling

The terrain and self-gradient corrected **G_{NE}** and **G_{UV}** data are tie line levelled across the entire survey using a least-squares minimisation of differences at survey line intersections. Occasionally some micro-levelling might be performed.

8.10 Transformation into GDD & g_D

The transformation of the measured, corrected, and levelled **G_{NE}** and **G_{UV}** data into gravity and components of the full gravity gradient tensor is accomplished using two methods:

- Fourier domain transformation
- Equivalent source transformation

The input data for the Fourier method are the average NE and UV components computed from the complement data, as described in section 8.3. The Fourier method relies on the Fourier transform of Laplace's equation. The application of this transform to the complex function **G_{NE} + i G_{UV}** provides a stable and accurate calculation of each of the full tensor components and gravity. The Fourier method performs piece-wise upward and downward continuation to work with data collected on a surface that varies from a flat horizontal plane. For stability of the downward continuation, the data are low-pass filtered. The cut-off wavelength of this filter depends on the variations in altitude range and line spacing. It is set to the smallest value that provides stable downward continuation.

In survey areas where the variability of the terrain surface (and hence the flight surface) makes it impossible to obtain Fourier transformation results that are both high resolution and stable, an alternate method can be applied which bypasses the upward and downward continuation steps. The results are calculated at the flight surface. This approach lacks the mathematical rigour of the complete method but allows for greater detail in the output data. It must be noted however that, if the terrain is too extreme, this method may fail to accurately transform the input data. This can be checked by comparing the input **G_{NE}** and **G_{UV}** data with the predicted values of the same data after transformation. If they do not match well, the Fourier transformation method cannot be relied upon.

The input data for the equivalent source method are the individual NE and UV component data from each complement, as referred to in section 8.3. The equivalent source method relies on a smooth model inversion to calculate the density of a surface of sources and from these sources, a forward calculation provides the **GDD** and **g_D** data as well as the other gradient tensor components. The effect of the smoothing is similar to but not the same as the application of the low-pass filter in the Fourier domain method. In areas of highly variable terrain, flying low can lead to some instability in the equivalent source method as the computation surface approaches the location of the derived sources. It may be necessary to accept some localised instability in order to optimise the overall result.

The equivalent source procedure defines an array of rectangular (usually square) plates, extending slightly past the survey area in all directions. Each plate is assumed to have uniform (but initially unknown) surface density and to lie on a predefined solution surface. Using the individual NE and UV component data measured at the centre of each plate, a system of linear equations is formed which can then be solved for the density of each plate using a least squares inversion method. Once the plate density distribution is determined, it can be used for forward calculation of all tensor components and of vertical gravity.

The limitations of gravity gradiometry in reconstructing the long wavelengths of gravity can lead to differences in the results of these two methods at long wavelength. The merging of the **g_D** data with externally supplied regional gravity such as the DTU13 gravity provides a way of reducing these differences. The application of this procedure will depend on the survey size and resolution of available regional gravity. If survey size is too small or regional gravity resolution too large, regional conforming is not applied.

8.11 Terrain Corrections Using Alternate Terrain Densities

Although both uncorrected processed and transformed data and unit density terrain correction data are supplied, it is not recommended that these be used to create final data corrected for any arbitrary terrain correction density. The principal reason for this is that tie line levelling occurs after application of the terrain correction. As a result, levelling errors present in the terrain correction channels by virtue of positional inaccuracy are not removed from these channels and will be present in any data corrected with them. Further, filtering applied in creating the uncorrected, transformed data is not applied to the terrain correction channels. Mixing data filtered in different ways is not advised.

An alternative method (valid only for datasets where waterbody(ies) have not been taken into account when computing the terrain corrections) uses the linear relationship between the terrain corrections at different densities and the corresponding gravity gradient or g_{DD} values. This method can be applied to either the grid data or the located data. An example is given using G_{DD} :

The new density is referred to as ρ_N , the existing densities as ρ_1 and ρ_2

$$g_{DD}(\rho_N) = g_{DD}(\rho_1) + (g_{DD}(\rho_2) - g_{DD}(\rho_1)) \times \frac{(\rho_N - \rho_1)}{(\rho_2 - \rho_1)}$$

Note that the terrain correction channel is eliminated by substitution in deriving this equation.

It is recommended that two densities that differ by a reasonable value be used for this method, in order to minimise uncertainties caused by noise in the data. The values of 0.00 and 2.67 g/cm³ usually delivered should be sufficient to yield useful results.

8.12 Noise & Signal

By taking two independent measurements of the NE and UV curvature components at each sample point, it is possible to obtain a direct indication of the reliability of these measurements. The standard deviation of half the difference of the pairs of measurements - (A_{NE}, B_{NE}) and (A_{UV}, B_{UV}) - provides a good estimate of the survey noise:

$$Noise_{NE} = StdDev\left(\frac{(A_{NE} - B_{NE})}{2}\right)$$

$$Noise_{UV} = StdDev\left(\frac{(A_{UV} - B_{UV})}{2}\right)$$

These difference channels are calculated for each data point. The standard deviation across all data points is the figure quoted for the survey as a whole.

This difference error has been demonstrated to follow a 'normal' or Gaussian statistical distribution, with a mean of zero. Therefore, the bulk of the population (95%) will lie between -2σ and $+2\sigma$ of the mean. For a typical survey noise estimate of, say, 3 E, 95% of the noise will be between -6 E and +6 E.

These typical errors in the curvature gradients translate to errors in G_{DD} of about 5 E and in g_D (in the shorter wavelengths) in the order of 0.1 mGal.

8.13 Risk Criteria in Interpretation

The risks associated with a **FALCON**[®] AGG survey are mainly controlled by the following factors.

- **Survey edge anomalies** – the transformation from measured curvature gradients to vertical gradient and vertical gravity gradient is subject to edge effects. Hence, any anomalies located within about 2 x line spacing of the edge of the survey boundaries should be treated with caution.
- **Single line anomalies** – for a wide-spaced survey, an anomaly may be present on only one line. Although it might be a genuine anomaly, the interpreter should note that no two-dimensional control can be applied.
- **Low amplitude (less than 2 σ) anomalies** – Are within the noise envelope and need to be treated with caution if they are single line anomalies and close in diameter to the cut-off wavelengths used.
- **Residual topographic error anomalies** – Inaccurate topographic correction either due to inaccurate DTM or local terrain density variations may produce anomalies. Comparing the DTM with the G_{DD} map terrain-corrected for different densities is a reliable way to confirm the legitimacy of an anomaly.
- **The low density of water and lake sediments** – (if present) can create significant gravity and gravity gradient lows, which may be unrelated to bedrock geology. It is recommended that all anomalies located within lakes or under water be treated with caution and assessed with bathymetry if available.

8.14 References

Boggs, D. B. and Dransfield, M. H., 2004, Analysis of errors in gravity derived from the Falcon[®] airborne gravity gradiometer, Lane, R. (ed.), Airborne Gravity 2004 - Abstracts from the ASEG-PESA Airborne Gravity 2004 Workshop, Geoscience Australia Record 2004/18, 135-141.

Christensen A.N., Dransfield, M. H. and Van Galder C, 2015, Noise and repeatability of airborne gravity gradiometry, First Break, Volume 33, April 2015, 55 - 63.

Dransfield, M. H., 2010, Conforming Falcon gravity and the global gravity anomaly, Geophysical Prospecting, 58, 469-483.

Dransfield, M. H. and Lee, J. B., 2004, The FALCON[®] airborne gravity gradiometer survey systems, Lane, R. (ed.), Airborne Gravity 2004 - Abstracts from the ASEG-PESA Airborne Gravity 2004 Workshop, Geoscience Australia Record 2004/18, 15-19.

Dransfield, M. H. and Zeng, Y., Airborne gravity gradiometry: terrain corrections and elevation error, Geophysics 2009/Sep 74(5).

Lee, J. B., 2001, FALCON Gravity Gradiometer Technology, Exploration Geophysics, 32, 75-79.

Lee, J. B.; Liu, G.; Rose, M.; Dransfield, M.; Mahanta, A.; Christensen, A. and Stone, P., 2001, High resolution gravity surveys from a fixed wing aircraft, Geoscience and Remote Sensing Symposium, 2001. IGARSS '01. IEEE 2001 International, 3, 1327-1331.

Stone, P. M. and Simsky, A., 2001, Constructing high resolution DEMs from Airborne Laser Scanner Data, Preview, Extended Abstracts: ASEG 15th Geophysical Conference and Exhibition, August 2001, Brisbane, 93, 99.

9 APPENDIX IV - DAILY REPORT

PROJECT NUMBER (XCALIBUR): 2400019					PROJECT MANAGER(S): Brett Robinson			
PROJECT NAME: Snow Lake					CREW LEADER(S): Abbas Malik			
CLIENT: Natural Resources Canada (NRCAN)					PROCESSOR(S): Paris Cassidy			
BASE OF OPERATIONS: Snow Lake, MB					OPERATOR(S): Abbas Malik			
TOTAL LINE KM: 8920.8					PILOT(S): Jesse Clayton, Ryan Linto, Stephen Parks			
ACCEPTED KM / % COMPLETE: 8920.8 / 100.0 %					AME(S): Allan Ott			
REMAINING: 0.0					OTHERS (S):			
DATE	DAY	FLIGHT NUMBER	AREA FLOWN	AIRCRAFT	PRODUCTION			COMMENTS <small>General Activities (problems, safety, crew movements, etc.)</small>
					FLOWN	ACCEPTED	STANDBY	
2024/03/13	Wed	No Flight		N869XA				Abbas and Allan on route to Flin Flon. Overnight in Winnipeg
2024/03/14	Thu	Ferry		N869XA				Crew and N869XA arrived on site spoke to airport manager, found a place to store spare on airport property and parking spot for the plane.
2024/03/15	Fri			N869XA				System startup in process, GPS base station is setup and ATP 2 sent for approval.
2024/03/16	Sat	001	Snow Lake	N869XA	724.8	724.8		One production flight for today, windy day, late start in the morning.
2024/03/17	Sun	002	Snow Lake	N869XA	735.2	684.8		
2024/03/17	Sun	003	Snow Lake	N869XA	845.6	845.6		Two Production flights for today.
2024/03/18	Mon	004	Snow Lake	N869XA	60.4			FOM, Laser cal done, and one production line was flown. Windy conditions. Flight aborted due to winds after one line. Weekly safety meeting held.
2024/03/19	Tue	005	Snow Lake	N869XA	724.8	543.6		One Production flights for today. High winds throughout the day no second flight possible. S.Parks off site. Line 10900, East end 100m high over tower.
2024/03/20	Wed	006	Snow Lake	N869XA	845.6	845.6		
2024/03/20	Wed	007	Snow Lake	N869XA	845.6	845.6		Two Production flights for today. Flying condition for today turbulence was moderate.
2024/03/21	Thu	008	Snow Lake	N869XA	845.6	845.6		
2024/03/21	Thu	009	Snow Lake	N869XA	161.2	110.8		Three productions flights for today. Flying condition for today turbulence was moderate to light. Abhi.G arrived on site.
2024/03/21	Thu	010	Snow Lake	N869XA	514.0	413.2		
2024/03/22	Fri	011	Snow Lake	N869XA	724.8	664.4		Two Production flights for today. Flying condition for today turbulence was moderate. Frank and Phuong arrive on site for client visit.
2024/03/22	Fri	012	Snow Lake	N869XA	724.8	664.4		
2024/03/23	Sat	013	Snow Lake	N869XA	724.8	724.8		Two Production flights for today and re-flight lines. Flying condition for today turbulence was light to moderate.
2024/03/23	Sat	014	Snow Lake	N869XA	655.2	655.2		
2024/03/24	Sun	015	Snow Lake	N869XA	352.4	352.4		Two Production flights for today. Flying condition for today turbulence was light to moderate.
2024/03/24	Sun	016	Snow Lake	N869XA				
2024/03/25	Mon	017	Snow Lake	N869XA				One production flight for today, Full coverage of the block and all re-flight lines are now flown.
2024/03/26	Tue		Snow Lake	N869XA				869 on its way to ottawa, Jesse.C and Ryan.L off site. System shutdown and foamed last night, spare packed.

PROJECT NUMBER (XCALIBUR):		2400019		AVERAGE DAY/NIGHT COSTS (inc. Taxes)									
PROJECT NAME:		Snow Lake											
CLIENT:		Natural Resources Canada (NRCan)		Hotel		\$ 200.00		Airport Storage					
BASE OF OPERATIONS:		Snow Lake, MB		Meals (Per Diems)		\$ 95.00		Jet Fuel + Airport Fees + Storage		Variable			
TOTAL LINE KM:		8920.8		Truck Rental		\$ 240.00		Other		Various			
ACCEPTED KM / % COMPLETE:		8920.8 / 100.0 %											
REMAINING:		0.0											
				TOTALS:	\$ 13,000.00	\$ 6,175.00	\$ 3,360.00	\$ -	18456.0	\$ 45,206.20	\$ 4,897.00	TOTAL = \$91,094.20	
DATE	DAY	FLIGHT NUMBER	AREA FLOWN	AIRCRAFT	# ROOMS IN FLIN FLON	HOTEL COST	MEALS (PER DIEM)	TRUCK COST	STORAGE COST	LITRES JET	JET FUEL COST	OTHER COSTS	NOTE
2024/03/13	Wed	No Flight		N869XA	2	\$ 400.00	\$ 190.00	\$ 240.00	\$ -	0.0	\$ -	\$ 2,397.00	Shipping Gear to Flin Flon via Manitoulin
2024/03/14	Thu	Ferry		N869XA	5	\$ 1,000.00	\$ 475.00	\$ -	\$ -	1082.0	\$ 2,680.72	\$ -	
2024/03/15	Fri			N869XA	5	\$ 1,000.00	\$ 475.00	\$ 240.00	\$ -	971.0	\$ 2,413.82	\$ -	
2024/03/16	Sat	001	Snow Lake	N869XA	5	\$ 1,000.00	\$ 475.00	\$ 240.00	\$ -	1107.0	\$ 2,996.43	\$ -	
2024/03/17	Sun	002	Snow Lake	N869XA	5	\$ 1,000.00	\$ 475.00	\$ 240.00	\$ -	1115.0	\$ 2,741.39	\$ -	
2024/03/17	Sun	003	Snow Lake	N869XA	5	\$ 1,000.00	\$ 475.00	\$ 240.00	\$ -	1082.0	\$ 2,680.72	\$ -	
2024/03/18	Mon	004	Snow Lake	N869XA	5	\$ 1,000.00	\$ 475.00	\$ 240.00	\$ -	597.0	\$ 1,495.86	\$ -	
2024/03/19	Tue	005	Snow Lake	N869XA	4	\$ 800.00	\$ 380.00	\$ 240.00	\$ -	1066.0	\$ 2,642.25	\$ -	
2024/03/20	Wed	006	Snow Lake	N869XA	4	\$ 800.00	\$ 380.00	\$ 240.00	\$ -	1131.0	\$ 2,769.95	\$ -	
2024/03/20	Wed	007	Snow Lake	N869XA	4	\$ 800.00	\$ 380.00	\$ 240.00	\$ -	1110.0	\$ 2,717.24	\$ -	
2024/03/21	Thu	008	Snow Lake	N869XA	5	\$ 1,000.00	\$ 475.00	\$ 240.00	\$ -	1132.0	\$ 2,689.16	\$ -	
2024/03/21	Thu	009	Snow Lake	N869XA	5	\$ 1,000.00	\$ 475.00	\$ 240.00	\$ -	488.0	\$ 1,122.69	\$ -	
2024/03/21	Thu	010	Snow Lake	N869XA	5	\$ 1,000.00	\$ 475.00	\$ 240.00	\$ -	793.0	\$ 1,927.54	\$ -	
2024/03/22	Fri	011	Snow Lake	N869XA	5	\$ 1,000.00	\$ 475.00	\$ 240.00	\$ -	1035.0	\$ 2,444.37	\$ -	
2024/03/22	Fri	012	Snow Lake	N869XA	5	\$ 1,000.00	\$ 475.00	\$ 240.00	\$ -	986.0	\$ 2,358.74	\$ -	
2024/03/23	Sat	013	Snow Lake	N869XA	5	\$ 1,000.00	\$ 475.00	\$ 240.00	\$ -	1094.0	\$ 2,727.92	\$ -	
2024/03/23	Sat	014	Snow Lake	N869XA	5	\$ 1,000.00	\$ 475.00	\$ 240.00	\$ -	986.0	\$ 2,330.15	\$ -	
2024/03/24	Sun	015	Snow Lake	N869XA	5	\$ 1,000.00	\$ 475.00	\$ 240.00	\$ -	1129.0	\$ 2,663.48	\$ -	
2024/03/24	Sun	016	Snow Lake	N869XA	5	\$ 1,000.00	\$ 475.00	\$ 240.00	\$ -	1060.0	\$ 2,531.24	\$ -	
2024/03/25	Mon	017	Snow Lake	N869XA	5	\$ 1,000.00	\$ 475.00	\$ 240.00	\$ -	512.0	\$ 1,272.53	\$ -	
2024/03/26	Tue		Snow Lake	N869XA	5	\$ 1,000.00	\$ 475.00	\$ 240.00	\$ -	0.0	\$ -	\$ 2,500.00	Shipping gear to Ottawa via Manitoulin

10 APPENDIX V - CALIBRATIONS

10.1 Self-gradient Calibration

The **FALCON**[®] AGG System is sensitive to gravity gradients due to the mass of the aircraft and the equipment around it. As the aircraft's angular attitude changes, these gravity gradients change, causing a changing self-gradient signal to be recorded by the **FALCON**[®] AGG. The self-gradient calibrations flights are performed in order to calibrate the effect of these masses against aircraft attitude so that they can be removed in the processing of the survey.

The values and further specifications of the self-gradient calibration cannot be released due to ITAR restrictions.

10.2 Laser Scanner Calibration

The laser scanner calibration is performed after installation or adjustment of the laser scanner. The calibration is used to refine the lever arm offsets and calculate the pointing offsets of the scanner, GPS, and **FALCON**[®] AGG platform. The calibration takes about fifteen minutes. The aircraft flies at a constant heading and a constant altitude of 250 feet above flat topography. Six cycles of +/-10° roll manoeuvres at a period of five seconds are performed, followed by six cycles of +/-10° pitch manoeuvres at a period of five seconds, and finally one minute of combination pitch and roll manoeuvres to simulate turbulence. These manoeuvres are then repeated at 500 feet altitude.

11 APPENDIX VI - FINAL PRODUCTS

Final **FALCON**[®] AGG digital line data were provided in an 8 Hz Geosoft Oasis GDB database file containing the fields and format described in *Table 4* below.

Grids of AGG products, as well as the DTM, were delivered, as described in *Table 5* below. The grids are in Geosoft GRD format with grid cell size of 100 m, with the exception of the DTM grids, which have a 15 m cell size.

One copy of the digital archives was delivered along with a copy of this Logistics and Processing Report.

Variable Name	Description	Units
LINE	Line Number	
FLIGHT	Flight Number	-
DATE	Flight Date	yyyymmdd
UTCTIME	UTCTIME = Universal Time (seconds since midnight)	seconds
UTC_1980	Universal Time (seconds since January 6 1980)	seconds
FIDCOUNT	Fiducial	8 Hz
LAT	Latitude in NAD83	degrees

LONG	Longitude in NAD83	degrees
EASTING	Easting (X) in NAD83 UTM Zone 14N	m
NORTHING	Northing (Y) in NAD83 UTM Zone 14N	m
SURFACE	Drape flying surface (Referenced to Mean Sea Level)	metres
GPSALT	Differentially corrected GPS altitude (MSL)	metres
TANDEM_X	Raw TanDEM-X (MSL)	metres
LALT	Calculated laser scanner clearance (GPSALT - DEMLEV)	metres
DEMLEV	Scanner Refined Digital Elevation Model (MSL)	metres
TURBULENCE_VERT	Estimated vertical platform turbulence (vertical acceleration where $g = 9.80665 \text{ m/sec/sec}$)	millig
ROLL	Aircraft roll	deg
PITCH	Aircraft pitch	deg
YAW	Aircraft yaw	deg
NOISE_Gne	NE gradient uncorrelated noise estimate after levelling	Eötvös
NOISE_Guv	UV gradient uncorrelated noise estimate after levelling	Eötvös
ANE_0p0_PRELIM	Preliminary measured A complement GNE gravity gradient not terrain corrected	Eötvös
AUV_0p0_PRELIM	Preliminary measured A complement GUV gravity gradient not terrain corrected	Eötvös
BNE_0p0_PRELIM	Preliminary measured B complement GNE gravity gradient not terrain corrected	Eötvös
BUV_0p0_PRELIM	Preliminary measured B complement GUV gravity gradient not terrain corrected	Eötvös
TERRAIN_COR_Gdd	Terrain effect calculated for DD using a density of 1 g/cc	Eötvös
TERRAIN_COR_Gne	Terrain effect calculated for NE using a density of 1 g/cc	Eötvös
TERRAIN_COR_Guv	Terrain effect calculated for UV using a density of 1 g/cc	Eötvös
GRAV_A_Gne_2p67	Self gradient & terrain corrected NE gradient using terrain correction density 2.67 g/cc	Eötvös
GRAV_A_Guv_2p67	Self gradient & terrain corrected UV gradient using terrain correction density 2.67 g/cc	Eötvös
GRAV_B_Gne_2p67	Self gradient & terrain corrected NE gradient using terrain correction density 2.67 g/cc	Eötvös
GRAV_B_Guv_2p67	Self gradient & terrain corrected UV gradient using terrain correction density 2.67 g/cc	Eötvös
GRAV_A_Gne_0	Self gradient corrected NE gradient no terrain correction	Eötvös
GRAV_A_Guv_0	Self gradient corrected UV gradient no terrain correction	Eötvös
GRAV_B_Gne_0	Self gradient corrected NE gradient no terrain correction	Eötvös
GRAV_B_Guv_0	Self gradient corrected UV gradient no terrain correction	Eötvös
DRAPE_EQS	Equivalent Source drape surface (smoothed altitude)	metres
GRAV_Gd_EQS_2p67	Equivalent Source derived vertical gravity using terrain correction density 2.67 g/cc	mGal
GRAV_Gd_EQS_2p67_C	Equivalent Source derived vertical gravity using terrain correction density 2.67 g/cc conformed to DTU13 Regional gravity	mGal
GRAV_Gee_EQS_2p67	Equivalent Source derived Gee gradient using terrain correction density 2.67 g/cc	Eötvös
GRAV_Gnn_EQS_2p67	Equivalent Source derived Gnn gradient using terrain correction density 2.67 g/cc	Eötvös

GRAV_Gdd_EQS_2p67	Equivalent Source derived vertical gravity gradient using terrain correction density 2.67 g/cc	Eötvös
GRAV_Gdd_EQS_2p67_C	Equivalent Source derived vertical gravity gradient using terrain correction density 2.67 g/cc conformed to DTU13 Regional gravity	Eötvös
GRAV_Ged_EQS_2p67	Equivalent Source derived Ged horizontal EW gradient using terrain correction density 2.67 g/cc	Eötvös
GRAV_Gnd_EQS_2p67	Equivalent Source derived Gnd horizontal NS gradient using terrain correction density 2.67 g/cc	Eötvös
GRAV_Gne_EQS_2p67	Equivalent Source derived Gne curvature gradient using terrain correction density 2.67 g/cc	Eötvös
GRAV_Guv_EQS_2p67	Equivalent Source derived Guv curvature gradient using terrain correction density 2.67 g/cc	Eötvös
GRAV_Gd_EQS_0	Equivalent Source derived vertical gravity no terrain correction	mGal
GRAV_Gd_EQS_0_C	Equivalent Source derived vertical gravity no terrain correction conformed to DTU13 Regional gravity	mGal
GRAV_Gee_EQS_0	Equivalent Source derived Gee gradient no terrain correction	Eötvös
GRAV_Gnn_EQS_0	Equivalent Source derived Gnn gradient no terrain correction	Eötvös
GRAV_Gdd_EQS_0	Equivalent Source derived vertical gravity gradient no terrain correction	Eötvös
GRAV_Gdd_EQS_0_C	Equivalent Source derived vertical gravity gradient no terrain correction conformed to DTU13 Regional gravity	Eötvös
GRAV_Ged_EQS_0	Equivalent Source derived Ged horizontal EW gradient no terrain correction	Eötvös
GRAV_Gnd_EQS_0	Equivalent Source derived Gnd horizontal NS gradient no terrain correction	Eötvös
GRAV_Gne_EQS_0	Equivalent Source derived Gne curvature gradient no terrain correction	Eötvös
GRAV_Guv_EQS_0	Equivalent Source derived Guv curvature gradient no terrain	Eötvös
GRAV_Gd_EQS_2p95	Equivalent Source derived vertical gravity using terrain correction density 2.95 g/cc	mGal
GRAV_Gd_EQS_2p95_C	Equivalent Source derived vertical gravity using terrain correction density 2.95 g/cc conformed to DTU13 Regional gravity	mGal
GRAV_Gee_EQS_2p95	Equivalent Source derived Gee gradient using terrain correction density 2.95 g/cc	Eötvös
GRAV_Gnn_EQS_2p95	Equivalent Source derived Gnn gradient using terrain correction density 2.95 g/cc	Eötvös
GRAV_Gdd_EQS_2p95	Equivalent Source derived vertical gravity gradient using terrain correction density 2.95 g/cc	Eötvös
GRAV_Gdd_EQS_2p95_C	Equivalent Source derived vertical gravity gradient using terrain correction density 2.95 g/cc conformed to DTU13 Regional gravity	Eötvös
GRAV_Ged_EQS_2p95	Equivalent Source derived Ged horizontal EW gradient using terrain correction density 2.95 g/cc	Eötvös
GRAV_Gnd_EQS_2p95	Equivalent Source derived Gnd horizontal NS gradient using terrain correction density 2.95 g/cc	Eötvös
GRAV_Gne_EQS_2p95	Equivalent Source derived Gne curvature gradient using terrain correction density 2.95 g/cc	Eötvös
GRAV_Guv_EQS_2p95	Equivalent Source derived Guv curvature gradient using terrain correction density 2.95 g/cc	Eötvös
GRAV_Gd_EQS_2p67_FILT	Enhanced Equivalent Source derived vertical gravity using terrain correction density 2.67 g/cc	mGal

GRAV_Gd_EQS_2p67_FILT_C	Enhanced Equivalent Source derived vertical gravity using terrain correction density 2.67 g/cc conformed to DTU13 Regional gravity	mGal
GRAV_Gee_EQS_2p67_FILT	Enhanced Equivalent Source derived Gee gradient using terrain correction density 2.67 g/cc	Eötvös
GRAV_Gnn_EQS_2p67_FILT	Enhanced Equivalent Source derived Gnn gradient using terrain correction density 2.67 g/cc	Eötvös
GRAV_Gdd_EQS_2p67_FILT	Enhanced Equivalent Source derived vertical gravity gradient using terrain correction density 2.67 g/cc	Eötvös
GRAV_Gdd_EQS_2p67_C	Equivalent Source derived vertical gravity gradient using terrain correction density 2.67 g/cc conformed to DTU13 Regional gravity	Eötvös
GRAV_Ged_EQS_2p67_FILT	Enhanced Equivalent Source derived Ged horizontal EW gradient using terrain correction density 2.67 g/cc	Eötvös
GRAV_Gnd_EQS_2p67_FILT	Enhanced Equivalent Source derived Gnd horizontal NS gradient using terrain correction density 2.67 g/cc	Eötvös
GRAV_Gne_EQS_2p67_FILT	Enhanced Equivalent Source derived Gne curvature gradient using terrain correction density 2.67 g/cc	Eötvös
GRAV_Guv_EQS_2p67_FILT	Enhanced Equivalent Source derived Guv curvature gradient using terrain correction density 2.67 g/cc	Eötvös
GRAV_Gd_EQS_0_FILT	Enhanced Equivalent Source derived vertical gravity no terrain correction	mGal
GRAV_Gd_EQS_0_FILT_C	Enhanced Equivalent Source derived vertical gravity no terrain correction conformed to DTU13 Regional gravity	mGal
GRAV_Gee_EQS_0_FILT	Enhanced Equivalent Source derived Gee gradient no terrain correction	Eötvös
GRAV_Gnn_EQS_0_FILT	Enhanced Equivalent Source derived Gnn gradient no terrain correction	Eötvös
GRAV_Gdd_EQS_0_FILT	Enhanced Equivalent Source derived vertical gravity gradient no terrain correction	Eötvös
GRAV_Gdd_EQS_0_FILT_C	Enhanced Equivalent Source derived vertical gravity gradient no terrain correction conformed to DTU13 Regional gravity	Eötvös
GRAV_Ged_EQS_0_FILT	Enhanced Equivalent Source derived Ged horizontal EW gradient no terrain correction	Eötvös
GRAV_Gnd_EQS_0_FILT	Enhanced Equivalent Source derived Gnd horizontal NS gradient no terrain correction	Eötvös
GRAV_Gne_EQS_0_FILT	Enhanced Equivalent Source derived Gne curvature gradient no terrain correction	Eötvös
GRAV_Guv_EQS_0_FILT	Enhanced Equivalent Source derived Guv curvature gradient no terrain correction	Eötvös
GRAV_Gd_EQS_2p95_FILT	Enhanced Equivalent Source derived vertical gravity using terrain correction density 2.95 g/cc	mGal
GRAV_Gd_EQS_2p95_FILT_C	Enhanced Equivalent Source derived vertical gravity using terrain correction density 2.95 g/cc conformed to DTU13 Regional gravity	mGal
GRAV_Gee_EQS_2p95_FILT	Enhanced Equivalent Source derived Gee gradient using terrain correction density 2.95 g/cc	Eötvös
GRAV_Gnn_EQS_2p95_FILT	Enhanced Equivalent Source derived Gnn gradient using terrain correction density 2.95 g/cc	Eötvös
GRAV_Gdd_EQS_2p95_FILT	Enhanced Equivalent Source derived vertical gravity gradient using terrain correction density 2.95 g/cc	Eötvös
GRAV_Gdd_EQS_2p95_FILT_C	Enhanced Equivalent Source derived vertical gravity gradient using terrain correction density 2.95 g/cc conformed to DTU13 Regional gravity	Eötvös

GRAV_Ged_EQS_2p95_FILT	Enhanced Equivalent Source derived Ged horizontal EW gradient using terrain correction density 2.95 g/cc	Eötvös
GRAV_Gnd_EQS_2p95_FILT	Enhanced Equivalent Source derived Gnd horizontal NS gradient using terrain correction density 2.95 g/cc	Eötvös
GRAV_Gne_EQS_2p95_FILT	Enhanced Equivalent Source derived Gne curvature gradient using terrain correction density 2.95 g/cc	Eötvös
GRAV_Guv_EQS_2p95_FILT	Enhanced Equivalent Source derived Guv curvature gradient using terrain correction density 2.95 g/cc	Eötvös
DRAPE_FFT	Fourier drape surface (smoothed altitude)	metres
GRAV_Gd_FFT_2p67_FILT	Enhanced Fourier derived vertical gravity using terrain correction density 2.67 g/cc	mGal
GRAV_Gd_FFT_2p67_FILT_C	DTU13 Conformed Enhanced Fourier derived vertical gravity using terrain correction density 2.67 g/cc	mGal
GRAV_Gee_FFT_2p67_FILT	Enhanced Fourier derived Gee gradient using terrain correction density 2.67 g/cc	Eötvös
GRAV_Gnn_FFT_2p67_FILT	Enhanced Fourier derived Gnn gradient using terrain correction density 2.67 g/cc	Eötvös
GRAV_Gdd_FFT_2p67_FILT	Enhanced Fourier derived vertical gravity gradient using terrain correction density 2.67 g/cc	Eötvös
GRAV_Gdd_FFT_2p67_FILT_C	Enhanced Fourier derived vertical gravity gradient using terrain correction density 2.67 g/cc conformed to DTU13 Regional gravity	Eötvös
GRAV_Ged_FFT_2p67_FILT	Enhanced Fourier derived Ged horizontal EW gradient using terrain correction density 2.67 g/cc	Eötvös
GRAV_Gnd_FFT_2p67_FILT	Enhanced Fourier derived Gnd horizontal NS gradient using terrain correction density 2.67 g/cc	Eötvös
GRAV_Gne_FFT_2p67_FILT	Enhanced Fourier derived Gne curvature gradient using terrain correction density 2.67 g/cc	Eötvös
GRAV_Guv_FFT_2p67_FILT	Enhanced Fourier derived Guv curvature gradient using terrain correction density 2.67 g/cc	Eötvös
GRAV_Gd_FFT_0_FILT	Enhanced Fourier derived vertical gravity no terrain correction	mGal
GRAV_Gd_FFT_0_FILT_C	DTU13 Conformed Enhanced Fourier derived vertical gravity no terrain correction	mGal
GRAV_Gee_FFT_0_FILT	Enhanced Fourier derived Gee gradient no terrain correction	Eötvös
GRAV_Gnn_FFT_0_FILT	Enhanced Fourier derived Gnn gradient no terrain correction	Eötvös
GRAV_Gdd_FFT_0_FILT	Enhanced Fourier derived vertical gravity gradient no terrain correction	Eötvös
GRAV_Gdd_FFT_0_FILT_C	Enhanced Fourier derived vertical gravity gradient no terrain correction conformed to DTU13 Regional gravity	Eötvös
GRAV_Ged_FFT_0_FILT	Enhanced Fourier derived Ged horizontal EW gradient no terrain correction	Eötvös
GRAV_Gnd_FFT_0_FILT	Enhanced Fourier derived Gnd horizontal NS gradient no terrain correction	Eötvös
GRAV_Gne_FFT_0_FILT	Enhanced Fourier derived Gne curvature gradient no terrain correction	Eötvös
GRAV_Guv_FFT_0_FILT	Enhanced Fourier derived Guv curvature gradient no terrain correction	Eötvös
GRAV_Gd_FFT_2p95_FILT	Enhanced Fourier derived vertical gravity using terrain correction density 2.95 g/cc	mGal
GRAV_Gd_FFT_2p95_FILT_C	Enhanced Fourier derived vertical gravity using terrain correction density 2.95 g/cc conformed to DTU13 Regional gravity	mGal

GRAV_Gee_FFT_2p95_FILT	Enhanced Fourier derived Gee gradient using terrain correction density 2.95 g/cc	Eötvös
GRAV_Gnn_FFT_2p95_FILT	Enhanced Fourier derived Gnn gradient using terrain correction density 2.95 g/cc	Eötvös
GRAV_Gdd_FFT_2p95_FILT	Enhanced Fourier derived vertical gravity gradient using terrain correction density 2.95 g/cc	Eötvös
GRAV_Gdd_FFT_2p95_FILT_C	Enhanced Fourier derived vertical gravity gradient using terrain correction density 2.95 g/cc conformed to DTU13 Regional gravity	Eötvös
GRAV_Ged_FFT_2p95_FILT	Enhanced Fourier derived Ged horizontal EW gradient using terrain correction density 2.95 g/cc	Eötvös
GRAV_Gnd_FFT_2p95_FILT	Enhanced Fourier derived Gnd horizontal NS gradient using terrain correction density 2.95 g/cc	Eötvös
GRAV_Gne_FFT_2p95_FILT	Enhanced Fourier derived Gne curvature gradient using terrain correction density 2.95 g/cc	Eötvös
GRAV_Guv_FFT_2p95_FILT	Enhanced Fourier derived Guv curvature gradient using terrain correction density 2.95 g/cc	Eötvös

 Table 4: Snow Lake Final FALCON[®] AGG Digital Data – Geosoft database format

File	Description	Units
2400019_DRAPE_EQS	Equivalent Source drape surface (smoothed altitude)	metres
2400019_DRAPE_FFT	Fourier drape surface (smoothed altitude)	metres
2400019_DTM_Full	Terrain (height above EGM96 geoid), 15 m grid cell, for final AGG processing	metres
2400019_DTM	Terrain (height above EGM96 geoid), 15 m grid cell (Trimmed for easy display)	metres
2400019_GRAV_Gd_EQS_0	Equivalent Source derived vertical gravity no terrain correction	mGal
2400019_GRAV_Gd_EQS_0_C	Equivalent Source derived vertical gravity no terrain correction conformed to DTU13 Regional gravity	mGal
2400019_GRAV_Gd_EQS_0_FILT	Enhanced Equivalent Source derived vertical gravity no terrain correction	mGal
2400019_GRAV_Gd_EQS_0_FILT_C	Enhanced Equivalent Source derived vertical gravity no terrain correction conformed to DTU13 Regional gravity	mGal
2400019_GRAV_Gd_EQS_2p67	Equivalent Source derived vertical gravity using terrain correction density 2.67 g/cc	mGal
2400019_GRAV_Gd_EQS_2p67_C	Equivalent Source derived vertical gravity using terrain correction density 2.67 g/cc conformed to DTU13 Regional gravity	mGal
2400019_GRAV_Gd_EQS_2p67_FILT	Enhanced Equivalent Source derived vertical gravity using terrain correction density 2.67 g/cc	mGal
2400019_GRAV_Gd_EQS_2p67_FILT_C	Enhanced Equivalent Source derived vertical gravity using terrain correction density 2.67 g/cc conformed to DTU13 Regional gravity	mGal
2400019_GRAV_Gd_EQS_2p95	Equivalent Source derived vertical gravity using terrain correction density 2.95 g/cc	mGal
2400019_GRAV_Gd_EQS_2p95_C	Equivalent Source derived vertical gravity using terrain correction density 2.95 g/cc conformed to DTU13 Regional gravity	mGal
2400019_GRAV_Gd_EQS_2p95_FILT	Enhanced Equivalent Source derived vertical gravity using terrain correction density 2.95 g/cc	mGal
2400019_GRAV_Gd_EQS_2p95_FILT_C	Enhanced Equivalent Source derived vertical gravity using terrain correction density 2.95 g/cc conformed to DTU13 Regional gravity	mGal
2400019_GRAV_Gd_FFT_0_FILT	Enhanced Fourier derived vertical gravity no terrain correction	mGal

2400019_GRAV_Gd_FFT_0_FILT_C	Enhanced Fourier derived vertical gravity no terrain correction conformed to DTU13 Regional gravity	mGal
2400019_GRAV_Gd_FFT_2P67_FILT	Enhanced Fourier derived vertical gravity using terrain correction density 2.67 g/cc	mGal
2400019_GRAV_Gd_FFT_2p67_FILT_C	Enhanced Fourier derived vertical gravity using terrain correction density 2.67 g/cc conformed to DTU13 Regional gravity	mGal
2400019_GRAV_Gd_FFT_2p95_FILT	Enhanced Fourier derived vertical gravity using terrain correction density 2.95 g/cc	mGal
2400019_GRAV_Gd_FFT_2p95_FILT_C	Enhanced Fourier derived vertical gravity using terrain correction density 2.95 g/cc conformed to DTU13 Regional gravity	mGal
2400019_GRAV_Gdd_EQS_0	Equivalent Source derived vertical gravity gradient no terrain correction	eotvos
2400019_GRAV_Gdd_EQS_0_C	Equivalent Source derived vertical gravity gradient no terrain correction conformed to DTU13 Regional gravity	eotvos
2400019_GRAV_Gdd_EQS_0_FILT	Enhanced Equivalent Source derived vertical gravity gradient no terrain correction	eotvos
2400019_GRAV_Gdd_EQS_0_FILT_C	Enhanced Equivalent Source derived vertical gravity gradient no terrain correction conformed to DTU13 Regional gravity	eotvos
2400019_GRAV_Gdd_EQS_2p67	Equivalent Source derived vertical gravity gradient using terrain correction density 2.67 g/cc	eotvos
2400019_GRAV_Gdd_EQS_2p67_C	Equivalent Source derived vertical gravity gradient using terrain correction density 2.67 g/cc conformed to DTU13 Regional gravity	eotvos
2400019_GRAV_Gdd_EQS_2p67_FILT	Enhanced Equivalent Source derived vertical gravity gradient using terrain correction density 2.67 g/cc	eotvos
2400019_GRAV_Gdd_EQS_2p67_FILT_C	Enhanced Equivalent Source derived vertical gravity gradient using terrain correction density 2.67 g/cc conformed to DTU13 Regional gravity	eotvos
2400019_GRAV_Gdd_EQS_2p95	Equivalent Source derived vertical gravity gradient using terrain correction density 2.95 g/cc	eotvos
2400019_GRAV_Gdd_EQS_2p95_C	Equivalent Source derived vertical gravity gradient using terrain correction density 2.95 g/cc conformed to DTU13 Regional gravity	eotvos
2400019_GRAV_Gdd_EQS_2p95_FILT	Enhanced Equivalent Source derived vertical gravity gradient using terrain correction density 2.95 g/cc	eotvos
2400019_GRAV_Gdd_EQS_2p95_FILT_C	Enhanced Equivalent Source derived vertical gravity gradient using terrain correction density 2.95 g/cc conformed to DTU13 Regional gravity	eotvos
2400019_GRAV_Gdd_FFT_0_FILT	Enhanced Fourier derived vertical gravity gradient no terrain correction	eotvos
2400019_GRAV_Gdd_FFT_0_FILT_C	Enhanced Fourier derived vertical gravity gradient no terrain correction conformed to DTU13 Regional gravity	eotvos
2400019_GRAV_Gdd_FFT_2P67_FILT	Enhanced Fourier derived vertical gravity gradient using terrain correction density 2.67 g/cc	eotvos
2400019_GRAV_Gdd_FFT_2p67_FILT_C	Enhanced Fourier derived vertical gravity gradient using terrain correction density 2.67 g/cc conformed to DTU13 Regional gravity	eotvos
2400019_GRAV_Gdd_FFT_2p95_FILT	Enhanced Fourier derived vertical gravity gradient using terrain correction density 2.95 g/cc	eotvos
2400019_GRAV_Gdd_FFT_2p95_FILT_C	Enhanced Fourier derived vertical gravity gradient using terrain correction density 2.95 g/cc conformed to DTU13 Regional gravity	eotvos
2400019_GRAV_Ged_EQS_0	Equivalent Source derived Ged horizontal EW gradient no terrain correction	eotvos
2400019_GRAV_Ged_EQS_0_FILT	Enhanced Equivalent Source derived Ged horizontal EW gradient no terrain correction	eotvos
2400019_GRAV_Ged_EQS_2p67	Equivalent Source derived Ged horizontal EW gradient using terrain correction density 2.67 g/cc	eotvos
2400019_GRAV_Ged_EQS_2p67_FILT	Enhanced Equivalent Source derived Ged horizontal EW gradient using terrain correction density 2.67 g/cc	eotvos
2400019_GRAV_Ged_EQS_2p95	Equivalent Source derived Ged horizontal EW gradient using terrain correction density 2.95 g/cc	eotvos
2400019_GRAV_Ged_EQS_2p95_FILT	Enhanced Equivalent Source derived Ged horizontal EW gradient using terrain correction density 2.95 g/cc	eotvos

2400019_GRAV_Ged_FFT_0_FILT	Enhanced Fourier derived Ged horizontal EW gradient no terrain correction	eotvos
2400019_GRAV_Ged_FFT_2P67_FILT	Enhanced Fourier derived Ged horizontal EW gradient using terrain correction density 2.67 g/cc	eotvos
2400019_GRAV_Ged_FFT_2p95_FILT	Enhanced Fourier derived Ged horizontal EW gradient using terrain correction density 2.95 g/cc	eotvos
2400019_GRAV_Gee_EQS_0	Equivalent Source derived Gee gradient no terrain correction	eotvos
2400019_GRAV_Gee_EQS_0_FILT	Enhanced Equivalent Source derived Gee gradient no terrain correction	eotvos
2400019_GRAV_Gee_EQS_2p67	Equivalent Source derived Gee gradient using terrain correction density 2.67 g/cc	eotvos
2400019_GRAV_Gee_EQS_2p67_FILT	Enhanced Equivalent Source derived Gee gradient using terrain correction density 2.67 g/cc	eotvos
2400019_GRAV_Gee_EQS_2p95	Equivalent Source derived Gee gradient using terrain correction density 2.95 g/cc	eotvos
2400019_GRAV_Gee_EQS_2p95_FILT	Enhanced Equivalent Source derived Gee gradient using terrain correction density 2.95 g/cc	eotvos
2400019_GRAV_Gee_FFT_0_FILT	Enhanced Fourier derived Gee gradient no terrain correction	eotvos
2400019_GRAV_Gee_FFT_2P67_FILT	Enhanced Fourier derived Gee gradient using terrain correction density 2.67 g/cc	eotvos
2400019_GRAV_Gee_FFT_2p95_FILT	Enhanced Fourier derived Gee gradient using terrain correction density 2.95 g/cc	eotvos
2400019_GRAV_Gnd_EQS_0	Equivalent Source derived Gnd horizontal NS gradient no terrain correction	eotvos
2400019_GRAV_Gnd_EQS_0_FILT	Enhanced Equivalent Source derived Gnd horizontal NS gradient no terrain correction	eotvos
2400019_GRAV_Gnd_EQS_2p67	Equivalent Source derived Gnd horizontal NS gradient using terrain correction density 2.67 g/cc	eotvos
2400019_GRAV_Gnd_EQS_2p67_FILT	Enhanced Equivalent Source derived Gnd horizontal NS gradient using terrain correction density 2.67 g/cc	eotvos
2400019_GRAV_Gnd_EQS_2p95	Equivalent Source derived Gnd horizontal NS gradient using terrain correction density 2.95 g/cc	eotvos
2400019_GRAV_Gnd_EQS_2p95_FILT	Enhanced Equivalent Source derived Gnd horizontal NS gradient using terrain correction density 2.95 g/cc	eotvos
2400019_GRAV_Gnd_FFT_0_FILT	Enhanced Fourier derived Gnd horizontal NS gradient no terrain correction	eotvos
2400019_GRAV_Gnd_FFT_2P67_FILT	Enhanced Fourier derived Gnd horizontal NS gradient using terrain correction density 2.67 g/cc	eotvos
2400019_GRAV_Gnd_FFT_2p95_FILT	Enhanced Fourier derived Gnd horizontal NS gradient using terrain correction density 2.95 g/cc	eotvos
2400019_GRAV_Gne_EQS_0	Equivalent Source derived Gne curvature gradient no terrain correction	eotvos
2400019_GRAV_Gne_EQS_0_FILT	Enhanced Equivalent Source derived Gne curvature gradient no terrain correction	eotvos
2400019_GRAV_Gne_EQS_2p67	Equivalent Source derived Gne curvature gradient using terrain correction density 2.67 g/cc	eotvos
2400019_GRAV_Gne_EQS_2p67_FILT	Enhanced Equivalent Source derived Gne curvature gradient using terrain correction density 2.67 g/cc	eotvos
2400019_GRAV_Gne_EQS_2p95	Equivalent Source derived Gne curvature gradient using terrain correction density 2.95 g/cc	eotvos
2400019_GRAV_Gne_EQS_2p95_FILT	Enhanced Equivalent Source derived Gne curvature gradient using terrain correction density 2.95 g/cc	eotvos
2400019_GRAV_Gne_FFT_0_FILT	Enhanced Fourier derived Gne curvature gradient no terrain correction	eotvos
2400019_GRAV_Gne_FFT_2P67_FILT	Enhanced Fourier derived Gne curvature gradient using terrain correction density 2.67 g/cc	eotvos
2400019_GRAV_Gne_FFT_2p95_FILT	Enhanced Fourier derived Gne curvature gradient using terrain correction density 2.95 g/cc	eotvos
2400019_GRAV_Gnn_EQS_0	Equivalent Source derived Gnn gradient no terrain correction	eotvos
2400019_GRAV_Gnn_EQS_0_FILT	Enhanced Equivalent Source derived Gnn gradient no terrain correction	eotvos
2400019_GRAV_Gnn_EQS_2p67	Equivalent Source derived Gnn gradient using terrain correction density 2.67 g/cc	eotvos
2400019_GRAV_Gnn_EQS_2p67_FILT	Enhanced Equivalent Source derived Gnn gradient using terrain correction density 2.67 g/cc	eotvos

2400019_GRAV_Gnn_EQS_2p95	Equivalent Source derived Gnn gradient using terrain correction density 2.95 g/cc	eotvos
2400019_GRAV_Gnn_EQS_2p95_FILT	Enhanced Equivalent Source derived Gnn gradient using terrain correction density 2.95 g/cc	eotvos
2400019_GRAV_Gnn_FFT_0_FILT	Enhanced Fourier derived Gnn gradient no terrain correction	eotvos
2400019_GRAV_Gnn_FFT_2P67_FILT	Enhanced Fourier derived Gnn gradient using terrain correction density 2.67 g/cc	eotvos
2400019_GRAV_Gnn_FFT_2p95_FILT	Enhanced Fourier derived Gnn gradient using terrain correction density 2.95 g/cc	eotvos
2400019_GRAV_Guv_EQS_0	Equivalent Source derived Guv curvature gradient no terrain	eotvos
2400019_GRAV_Guv_EQS_0_FILT	Enhanced Equivalent Source derived Guv curvature gradient no terrain correction	eotvos
2400019_GRAV_Guv_EQS_2p67	Equivalent Source derived Guv curvature gradient using terrain correction density 2.67 g/cc	eotvos
2400019_GRAV_Guv_EQS_2p67_FILT	Enhanced Equivalent Source derived Guv curvature gradient using terrain correction density 2.67 g/cc	eotvos
2400019_GRAV_Guv_EQS_2p95	Equivalent Source derived Guv curvature gradient using terrain correction density 2.95 g/cc	eotvos
2400019_GRAV_Guv_EQS_2p95_FILT	Enhanced Equivalent Source derived Guv curvature gradient using terrain correction density 2.95 g/cc	eotvos
2400019_GRAV_Guv_FFT_0_FILT	Enhanced Fourier derived Guv curvature gradient no terrain correction	eotvos
2400019_GRAV_Guv_FFT_2P67_FILT	Enhanced Fourier derived Guv curvature gradient using terrain correction density 2.67 g/cc	eotvos
2400019_GRAV_Guv_FFT_2p95_FILT	Enhanced Fourier derived Guv curvature gradient using terrain correction density 2.95 g/cc	eotvos

Table 5: Snow Lake Final FALCON[®] AGG Grids (Geosoft format)